

# Spectroscopic and *in vitro* Investigations of Fe<sup>2+</sup>/α-Ketoglutarate-Dependent Enzymes Involved in Nucleic Acid Repair and Modification

David Schmidl,<sup>[a]</sup> Niko S. W. Lindlar né Jonasson,<sup>[a]</sup> Annika Menke,<sup>[a]</sup> Sabine Schneider,<sup>[a]</sup> and Lena J. Daumann<sup>\*[a]</sup>

The activation of molecular oxygen for the highly selective functionalization and repair of DNA and RNA nucleobases is achieved by α-ketoglutarate (α-KG)/iron-dependent dioxygenases. Of special interest are the human homologues AlkBH of *Escherichia coli* EcAlkB and ten-eleven translocation (TET) enzymes. These enzymes are involved in demethylation or dealkylation of DNA and RNA, although additional physiological functions are continuously being found. Given their importance, studying enzyme-substrate interactions, turnover and kinetic parameters is pivotal for the understanding of the mode of action of these enzymes. Diverse analytical methods, including X-ray crystallography, UV/Vis absorption, electron paramagnetic


resonance (EPR), circular dichroism (CD) and nuclear magnetic resonance (NMR) spectroscopy have been employed to study the changes in the active site and the overall enzyme structure upon substrate, cofactor, and inhibitor addition. Several methods are now available to assess the activity of these enzymes. By discussing limitations and possibilities of these techniques for EcAlkB, AlkBH and TET we aim to give a comprehensive synopsis from a bioinorganic point-of-view, addressing researchers from different disciplines working in the highly interdisciplinary and rapidly evolving field of epigenetic processes and DNA/RNA repair and modification.

## 1. Introduction

In 1955 Hayaishi and Mason independently reported the existence of enzymes that use molecular oxygen (O<sub>2</sub>) to activate C–H bonds.<sup>[1]</sup> Remarkably, no potentially damaging reactive oxygen species (ROS) are formed during this process, which has raised interest in how the delicate task to activate molecular oxygen is handled in biology. Over the past 60 years, numerous enzymes with transition metal ion centers (Fe and Cu in particular) capable of controlled oxygen activation have been discovered. One important class, the non-heme iron enzymes such as the α-ketoglutarate- (α-KG) and Fe<sup>2+</sup>-dependent dioxygenases form a large superfamily and some members have been found to be pivotal for the modification and repair of biomolecules such as RNA and DNA. Two of the most investigated subfamilies to be discussed are the AlkB subfamily, particularly the bacterial EcAlkB and the nine homologues known in humans (AlkBH1-9), as well as the ten-eleven translocation (TET) enzyme subfamily with its three variants (TET1-3). All these enzymes are mostly involved in demethylation or dealkylation of proteins, DNA and/or RNA, although more

physiological functions have been, and will potentially be, revealed. Included in this review are only such AlkB homologues that act on RNA/DNA substrates. As the active site structure is strongly conserved among EcAlkB, AlkBH and TET, their reaction mechanisms are generally believed to be very similar, despite their large substrate scope. To study the mode of action and molecular recognition mechanisms of these enzymes, diverse analytical methods, including X-ray crystallography, UV/Vis and NMR spectroscopy or HPLC-MS techniques, have been employed. In this review, we provide an outline of important strategies used *in vitro* and summarize to what extent an insight into enzymatic structure and activity can be gained by their application. By discussing available data and conclusions for EcAlkB, AlkBH and TET we provide an extensive overview from a bioinorganic perspective, including aspects from the different interdisciplinary research areas addressing this rapidly evolving field of epigenetic processes and nucleic acid repair. In the present article, enzymes that incorporate both atoms of molecular dioxygen into organic molecules (either the substrate or α-KG) are referred to as “dioxygenases” and only their primary substrate beside α-KG is mentioned (α-KG is sometimes referred to as co-substrate, however, in this review, it will be considered a co-factor, in addition to Fe<sup>2+</sup>, to highlight the differences in substrates of the discussed enzymes). In contrast, enzymes which incorporate one oxygen atom into an organic substrate and the other atom is released as water are referred to as monooxygenases.

[a] D. Schmidl, N. S. W. Lindlar né Jonasson, A. Menke, Dr. S. Schneider, Prof. Dr. L. J. Daumann  
Department Chemie  
Ludwig-Maximilians-Universität München  
Butenandtstraße 5–13, 81377 München (Germany)  
E-mail: lena.daumann@lmu.de

 © 2022 The Authors. ChemBioChem published by Wiley-VCH GmbH. This is an open access article under the terms of the Creative Commons Attribution Non-Commercial NoDerivs License, which permits use and distribution in any medium, provided the original work is properly cited, the use is non-commercial and no modifications or adaptations are made.

### 1.1. Consensus mechanism of Fe<sup>2+</sup>/α-KG-dependent enzymes

For the superfamily of Fe<sup>2+</sup>/α-KG-dependent enzymes, a consensus mechanism has been formulated based on the work on bacterial taurine dioxygenase (TauD).<sup>[2]</sup> Variations of this mechanism, for example regarding the substrate and cofactor addition sequence, have been described.<sup>[3]</sup> Due to the lack of mechanistic data on the herein discussed EcAlkB, AlkBH, and TET enzymes, we present a summary of this consensus mechanism here, even though differences between the mechanisms of TauD on the one hand and EcAlkB/AlkBH/TET on the other hand are possible.

In this commonly accepted mechanism, the iron core is always coordinated by the so-called facial triad consisting of two histidine and one carboxylic acid (aspartate or glutamate) residues on one face of the coordination sphere, which is completed by three water ligands (Scheme 1, structure I). Subsequent coordination by α-KG replaces two water molecules (II). The last aqua ligand is displaced by uptake of a substrate R–H (III), which does not usually coordinate to the metal center, but rather is held close to the active site by the enzyme backbone. The free coordination site is then filled by molecular oxygen, which leads to the formation of a proposed iron(III)-superoxido species IV (in this article, the IUPAC nomenclature oxido, hydroxido, superoxido, etc., will be used in contrast to

the more common, but outdated, terms oxo, hydroxo, superoxo, etc.). These observations were mainly made *via* UV/Vis,<sup>[4]</sup> electron paramagnetic resonance (EPR),<sup>[5]</sup> and Mößbauer spectroscopy, often in combination with stopped-flow freeze-quench techniques. In addition, comparison of circular dichroism (CD) and magnetic circular dichroism (MCD) spectra collected from TauD with spectra of synthetic inorganic coordination compounds has given insight into the coordination chemistry of these enzymes.<sup>[6]</sup> The order of steps from I to IV is subject to some debate, as shown by a recent study by Solomon and co-workers on the coordination sequence in deacetoxycephalosporin C synthase (DAOCS, another enzyme of the Fe<sup>2+</sup>/α-KG superfamily).<sup>[3a]</sup> The superoxide in IV is proposed to react with the ketone carbon atom in α-KG to form the bridged peroxido species V. Loss of carbon dioxide generates the trigonal bipyramidal active iron(IV)-oxido species VI, which was first directly characterized in 2003 by Price and co-workers.<sup>[5]</sup> The nature of this compound was discovered by rapid freeze-quenching and subsequent Mößbauer measurements, and later by extended X-ray absorption fine structure (EXAFS) and resonance Raman studies.<sup>[2d,7]</sup> The iron(IV)-oxido species VI abstracts a hydrogen atom from the substrate resulting in the iron(III)-hydroxido species VII and a carbon-centered, organic radical R•.<sup>[4–5,8]</sup> In addition, Proshlyakov *et al.* used time-resolved Raman spectroscopy in conjunction with



David Schmidl received his B.Sc. and M.Sc. in Chemistry from the Ludwig-Maximilians-Universität (LMU) in Munich. After working with Prof. Theodor Agapie at California Institute of Technology (Pasadena) and in the chemical industry, he joined the laboratory of Prof. Lena J. Daumann at LMU in 2019 to work on a functional TET enzyme model complex and DNA cytosine modifications. He has been pursuing his Ph.D. degree at the University of Cambridge since October 2020, under the supervision of Prof. Sir Shankar Balasubramanian, exploring the chemical biology of the epigenome.



Niko S. W. Lindlar né Jonasson studied chemistry at the University of Heidelberg, Germany, at the Ludwig-Maximilians-Universität Munich, Germany, at Leopold-Franzens-Universität Innsbruck, Austria, and Harvard University, USA. He recently finished his Ph.D. on the use of functional model complexes for the study of iron(II)/α-keto acid dependent enzymes in the group of Prof. Lena Daumann at Ludwig-Maximilians-Universität, Germany.



Annika Menke completed her B.Sc. in a transnational chemistry program (Regio Chimica) at the Albert-Ludwig University of Freiburg and universit  de l'Haute Alsace Mulhouse, and prepared her Bachelor's thesis in the group of Prof. Weber. She conducted research internships in the groups of Prof. Newman at the university of Ottawa, Prof. Carell, and Prof. Daumann at the LMU before she began her

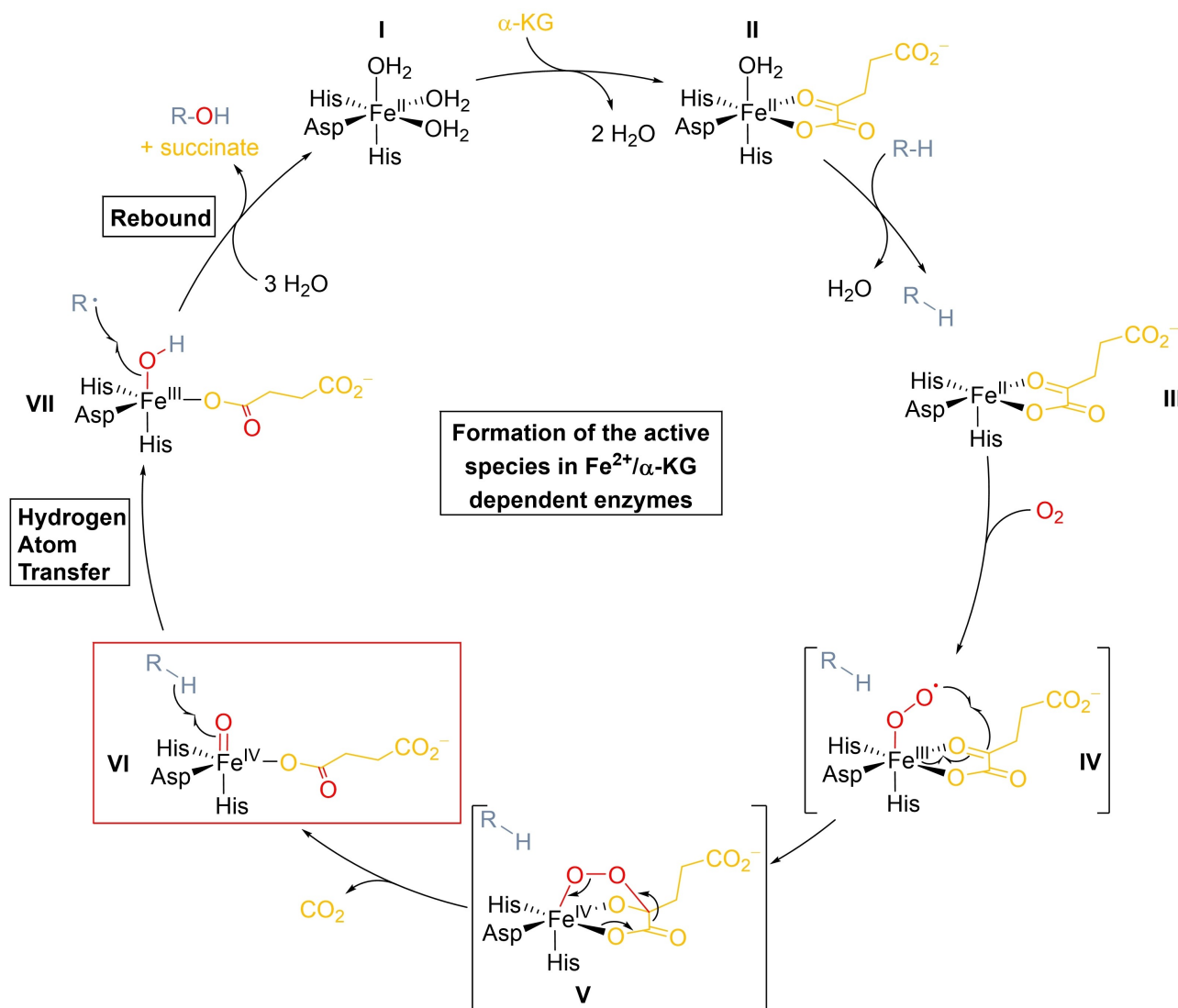


Master's thesis followed by her Ph.D. in the group of Prof. Daumann working on TET model complexes and their reactivity in epigenetics.

Sabine Schneider studied biology at the Ludwig-Maximilians University in Munich and conducted her Ph.D. at the University of Nottingham (UK). Following her postdoctoral work at the LMU, she started her independent research group at the Technical University Munich in 2010. In 2018 she became a Heisenberg fellow (DFG) and moved to the LMU Munich in 2019. Her research group uses molecular and chemical biology, biochemistry, and structural biology to investigate the molecular mechanism and function of structured nucleic acids and enzymes.



Lena Daumann studied chemistry at the University of Heidelberg and conducted her Ph.D. at the University of Queensland (Australia). Following postdoctoral stays at UC Berkeley and in Heidelberg she began her independent career at the LMU Munich in 2016. Her bioinorganic research group works on elucidating the role of lanthanides for bacteria as well as on iron enzymes and small biomimetic complexes that play a role in epigenetics and DNA repair.



**Scheme 1.** Consensus mechanism of an  $\text{Fe}^{2+}/\alpha\text{-KG}$ -dependent dioxygenase, the active species VI is highlighted in a red rectangle.<sup>[2]</sup> Species IV and V have not been observed directly but are often proposed as intermediates,<sup>[12]</sup> however, this is still a matter of discussion. R-H = substrate, R-OH = product.

stable isotope replacement ( $^{16}\text{O}/^{18}\text{O}$  and  $^1\text{H}/^2\text{H}$ ) to identify and characterize the iron species present during enzymatic catalysis. The authors detected the iron(IV)-oxido species VI, the iron(III)-hydroxido species VII as well as small amounts of a species consisting of the hydroxylated product coordinated to iron via the product's alcohol moiety.<sup>[9]</sup> The aforementioned hydrogen atom transfer (HAT) step from intermediate VI to VII is often, though not necessarily always, rate-limiting, which has been demonstrated in kinetic isotope effect (KIE) studies.<sup>[5,10]</sup> These two species finally react in a rebound-type reaction to produce the product R-OH and succinate, as well as regenerating the resting state I.

In a kinetic investigation of the enzyme factor inhibiting hypoxia inducible factors (FIHs), Knapp *et al.* studied the activation mechanism of such iron(II)/ $\alpha\text{-KG}$  dependent enzymes. Here, the authors found that whereas the mechanism itself is similar, the rate-limiting step is the formation of the bridged peroxido species instead of the reaction with the substrate,

which is to be expected, as FIHs are responsible for the sensing of oxygen.<sup>[11]</sup> This serves as an example that the mechanisms of different enzymes may show remarkable similarities in general but still differ in detail. Therefore, the presented mechanism should be viewed with caution and mechanistic work on EcAlkB, AlkBH and TET enzymes should be conducted.

## 1.2. Role in epigenetic processes, DNA repair and disease

The field of  $\text{Fe}^{2+}/\alpha\text{-KG}$ -dependent enzymes has seen considerable advances in the last decade and of increasing interest are the AlkBH and TET enzymes. These enzymes play important roles in gene regulation, epigenetic transformations and DNA repair, since they act on a wide range of alkylated nucleobases in DNA and RNA context. Table 1 presents an overview of the relevant enzymes and those involved in epigenetic processes. A

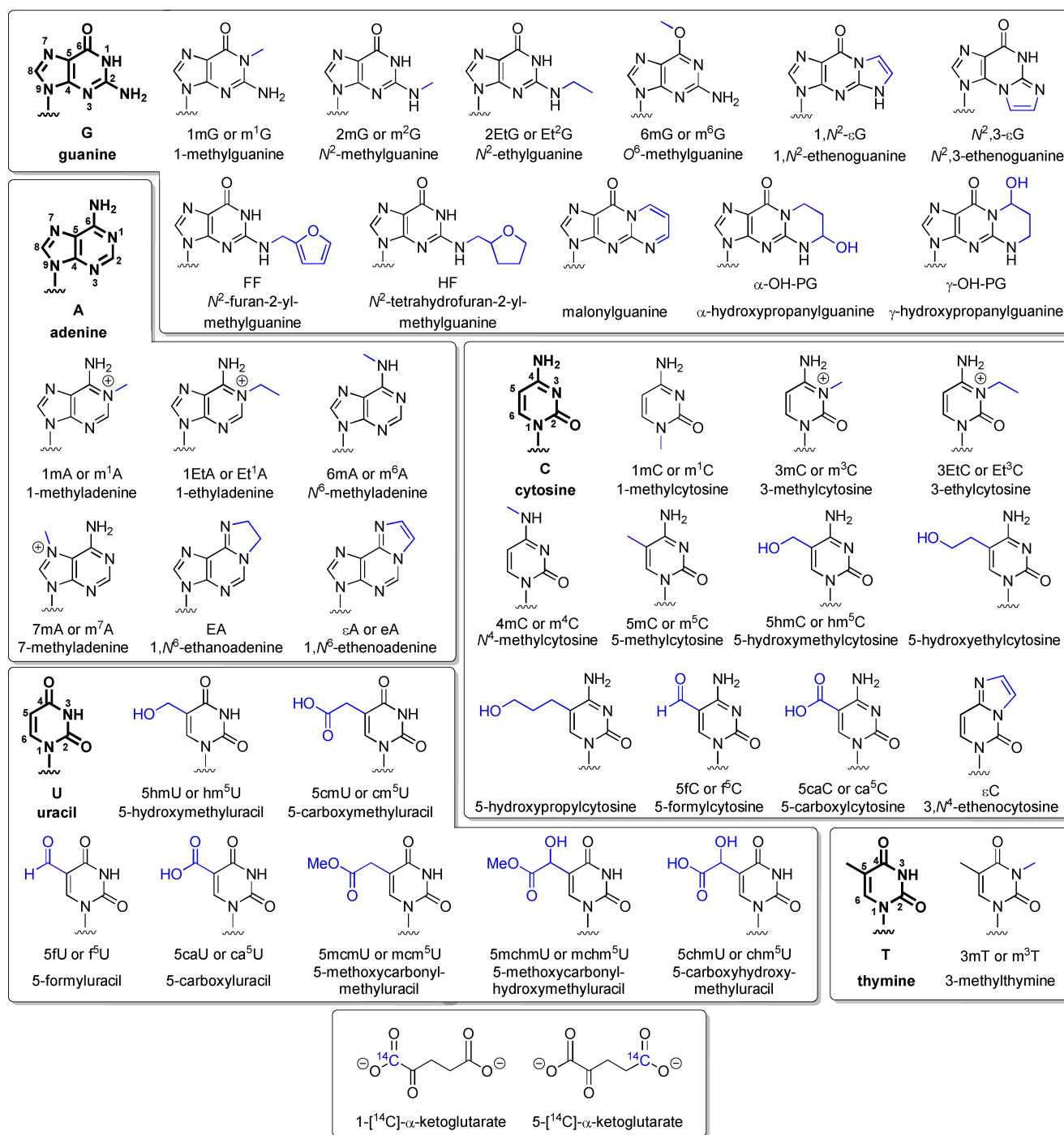
**Table 1.** Overview of discussed enzymes in this review with selected substrates and function. Please note for enzymes for which modified nucleobases in RNA as well as DNA were reported as substrates, only the modified base with non-superscript position descriptor is indicated, without differentiation between DNA or RNA. If only RNA is acted on, the modification position is indicated as superscript in line with the most commonly used nomenclature. However, TET-enzymes were shown to predominantly act on modified C in DNA, which is therefore indicated by using dC.

Enzyme	Selected substrates	Product	Function	References
EcAlkB	N-alkylated bases in DNA (ss preferred over ds) and RNA 1mA 3mC 3mT 1mG 6mA	Natural bases A C T G A	DNA repair	[14, 20]
AlkBH1	N-alkylated bases in ssDNA, mRNA and tRNA, alkylated histones, abasic sites in DNA  3mC 1mA 6mA 5mC Methylated histone H2A	Natural bases and proteins  C A A 5fC Histone H2A	RNA repair Histone dioxygenase Hydroxylase AP lyase <sup>[a]</sup>	[14, 20a, 20b, 21]
AlkBH2	N-alkylated bases in dsDNA and tRNA 3mC 1mA	Natural bases C A	DNA repair	[14, 20a, 20b, 20e, 22]
AlkBH3	Alkylated bases in ss DNA, ss RNA, tRNA, mRNA  3mC 1mA	  C A	Cell-type-dependent DNA repair Hydroxylation	[14, 20a, 20b, 20e, 20h, 22a, 22b, 23]
AlkBH5	mRNA m <sup>6</sup> A	Natural bases A	RNA demethylation	[14, 20a, 20b, 24]
AlkBH8	tRNA  cm <sup>5</sup> U	  mcm <sup>5</sup> U, (S)-mchm <sup>5</sup> U	Translation, tRNA hypermodification	[14, 20a, 20b, 25]
AlkBH9 <sup>[b]</sup>	mRNA (ss preferred over ds) m <sup>6</sup> A	Natural bases A	RNA demethylation	[14, 20a, 20b, 26]
TET1,2,3	Methylated bases in DNA  5mdC	Oxidizes bases in DNA 5hmdC, 5fdC, 5cadC	Regulation of epigenetically relevant DNA modifications	[27]

[a] Activity independent from Fe<sup>2+</sup> and  $\alpha$ -KG. [b] Also referred to as FTO (fat mass and obesity-associated protein).

summary of selected natural and *in vitro* used substrates and products, together with commonly used abbreviations, can be found in Scheme 2. Due to the direct interconnection of gene expression (alkylated substrates) and primary metabolic pathways (dioxygen and  $\alpha$ -KG co-substrates), these enzymes are often found to be involved in diseases. In addition, DNA hypermethylation of tumor suppressor gene promoters seems to be connected to hypoxia in tumors and a decreased function of TET enzymes in these tissues.<sup>[13]</sup> For individual mammalian AlkBH and TET enzymes, it has been shown that their loss-of-function as well as their aberrant expression and activities has an influence on various disease phenotypes, such as obesity, severe sensitivity to inflammation, multiple malformations, infertility and cancer.<sup>[14]</sup> This emphasizes the vital importance of these enzymes. Certain Fe<sup>2+</sup>/ $\alpha$ -KG-dependent enzymes, such as AlkBH1, are located in mitochondria next to enzymes that

participate in the tricarboxylic acid (TCA) cycle, the source of their essential cofactor  $\alpha$ -KG and their coproduct succinate. In the presence of oxygen, healthy cells utilize oxidative phosphorylation and the TCA cycle as controlled sources of basic metabolites and energy. In contrast, cancer cells adapt their metabolism to maximal cell growth through faster ATP production and redistribution of carbons towards nucleotide, protein and fatty acid synthesis by switching to high rates of glycolysis (= Warburg effect), even in the presence of oxygen.<sup>[15]</sup> Consequently, mutations in genes related to the TCA cycle have been associated with tumorigenesis, and cancer cells show altered concentrations of metabolites as well as accumulation of so-called oncometabolites.<sup>[16]</sup> For example, a mutation in the gene responsible for expressing isocitrate dehydrogenase leads to the generation of the novel oncometabolite 2-hydroxyglutamate (2-HG).<sup>[17]</sup> Due to the structural similarity between 2-HG and



**Scheme 2.** Overview of nucleobase substrates and products for Fe<sup>2+</sup>/α-KG dependent enzymes discussed herein. Please note, to enhance readability we did not differentiate between DNA and RNA. In addition, not all of these substrates necessarily represent the natural substrates of the mentioned enzymes.

α-KG, 2-HG is a competitive inhibitor of Fe<sup>2+</sup>/α-KG-dependent dioxygenases, such as TET enzymes and methyl-lysine demethylases.<sup>[16b,18]</sup> Thus, the inhibitory effect of oncometabolites on enzymes important for modulation of the epigenome and epitranscriptome directly links metabolic dysfunction to altered gene expression and oncogenesis.<sup>[19]</sup>

## 2. Structural Studies and Substrate Interactions

A variety of techniques are used to study the (*in vitro*) structure and function of the enzymes relevant for this review. This includes a detailed analysis of their backbone (backbone here refers to any structure of the enzyme excluding the metal binding site/enzyme coordination site or the co-factors) structure, their active sites/enzyme coordination site and the

nature of enzyme-substrate interactions. Figure 1 gives an overview of a simplified enzyme-cofactor-substrate complex, consisting of the enzyme backbone, the enzyme's coordination site (the so-called facial triad), the Fe central atom, the co-factor  $\alpha$ -KG (or succinate after oxidation of the iron center), dioxygen and the respective substrate or product. This review discusses the most important spectroscopic and spectrometric methods used to study the various parts of the enzyme-cofactor-substrate complex as well as the reactivity and kinetic properties of the aforementioned enzymes. The main focus lies on spectroscopic investigation of the enzyme backbone and active site as well as on techniques which assess enzyme reactivity by tracking the fate of substrates and/or products. It should be noted that there are more aspects contributing to a complete picture of the function of the enzyme in question than covered by this article. For instance, point mutations or deletion variants are very commonly included in activity studies to give indication for the function of particular amino acid residues. Also, hydrazines have recently been introduced as novel, versatile nucleophilic *in situ* probes for the study of (among others) AlkBH and related enzymes by activity-based protein profiling (ABPP).<sup>[28]</sup> While there are examples of these methods briefly introduced in several of the following sections where appropriate, this frequent element is not described as a technique in the context of this review in detail. Further, the mutual dependence between detailed *in vitro* investigation of an enzyme and experiments *in vivo* (e.g., by gene deletion studies to learn about its physiological function) is not addressed as *in vivo* studies are beyond the scope of this article.

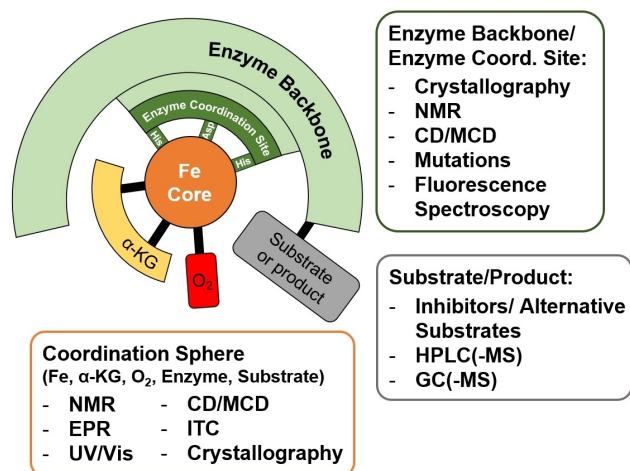


**Figure 1.** Overview of the methods used for the study of EcAlkB, AlkBH and TET discussed in this study. "Enzyme backbone" here refers to any structure of the enzyme excluding the metal binding site/enzyme coordination site or the co-factors).

## 2.1. Crystal structures

### Structure-function relationship of Fe<sup>2+</sup>/ $\alpha$ -KG dependent enzymes

Despite the low overall sequence identity of  $\alpha$ -KG-dependent enzymes (10–30%, between members of the AlkB-family and less than 10% between AlkB and TET enzymes), they consistently share the "jelly-roll" folding topology of the catalytic domain, made up of eight  $\beta$ -strands arranged in two four-stranded sheets (Figure 2A).<sup>[29]</sup> In addition, they have a minimal conserved binding motif for Fe<sup>2+</sup> and  $\alpha$ -KG in common, comprising of Asp-X<sub>x</sub>-His-X<sub>y</sub>-His-X<sub>z</sub>-Arg, which enables the catalytic reaction (Figure 2B, Scheme 1).

Crystal structures of EcAlkB (Figure 2B),<sup>[30]</sup> as well as eukaryotic AlkBH1,<sup>[31]</sup> AlkBH2,<sup>[30e,32]</sup> AlkBH3,<sup>[33]</sup> AlkBH5,<sup>[20d,34]</sup> AlkBH8,<sup>[35]</sup> AlkBH9,<sup>[36]</sup> TET1,<sup>[37]</sup> TET2<sup>[38]</sup> and the CXXC-domain of TET3<sup>[39]</sup> are available, some of them in complex with their substrate. Their differences in sequence, structural elements and accessory domains account for their remarkably large diversity in substrates and biological roles. Here, the binding interface (width of the cleft) and loop regions control access to the active site and determine the nature of the substrate the enzymes act on, such as dsDNA, ssDNA or RNA. Recently, a detailed review on the sequence and structural evolution of the AlkBH-family in respect to their substrate scope was published.<sup>[40]</sup> By substituting Fe<sup>2+</sup> and  $\alpha$ -KG with Mn<sup>2+</sup> and/or N-oxalylglycine (N-Ox), the latter being an broad-spectrum inhibitor of  $\alpha$ -KG-dependent oxygenases,<sup>[41]</sup> which occupy the same binding sites but do not allow substrate turnover, enables the elucidation of a structural snap-shot of substrate recognition by the oxygenases.<sup>[21d,34c,42]</sup> The first step in recognition of nucleobases with altered chemical structure (i.e. methylation, oxidatively damaged, etc.) in DNA or RNA by the dioxygenases occurs, as for most nucleic acid-binding proteins, by detection of changes in the local flexibility of the nucleic acid duplex, in duplex formation and in the stability of base pairing, which are induced by the altered nucleobase structures.<sup>[43]</sup> For example, m<sup>6</sup>A in RNA impedes RNA-duplex formation,<sup>[44]</sup> while 5mdC rigidifies the DNA backbone<sup>[45]</sup> and increases base pair stacking.<sup>[46]</sup> Substrate specificity is then further governed by molecular recognition through the residues lining the dioxygenase active site. For instance, EcAlkB has a broad substrate specificity and demethylates the predominant lesions 1-methyladenine (1mdA) and 3-methylcytosine (3mdC), as well as larger adducts, such as 1-ethyladenine and etheno-adducts in DNA.<sup>[20d,29a]</sup> Additionally, EcAlkB can use RNA as a substrate.<sup>[20i]</sup> There are about 30 X-ray crystal structures of EcAlkB alone and in complex with DNA containing various methylated or damaged nucleobases in the Protein Data Bank (PDB), providing insight into the enzyme's recognition mechanism.<sup>[30a-d,h]</sup> EcAlkB achieves this promiscuity by predominantly forming non-nucleobase-specific  $\pi$ -stacking interactions with the nucleobase through sandwiching it between Trp69 and His131 (Figure 2C). In contrast, TET1, TET2 and AlkBH9 act precisely on 5mdC, 5hmdC and m<sup>6</sup>A in DNA and RNA, respectively, by forming base-specific interactions as shown by the structures of their

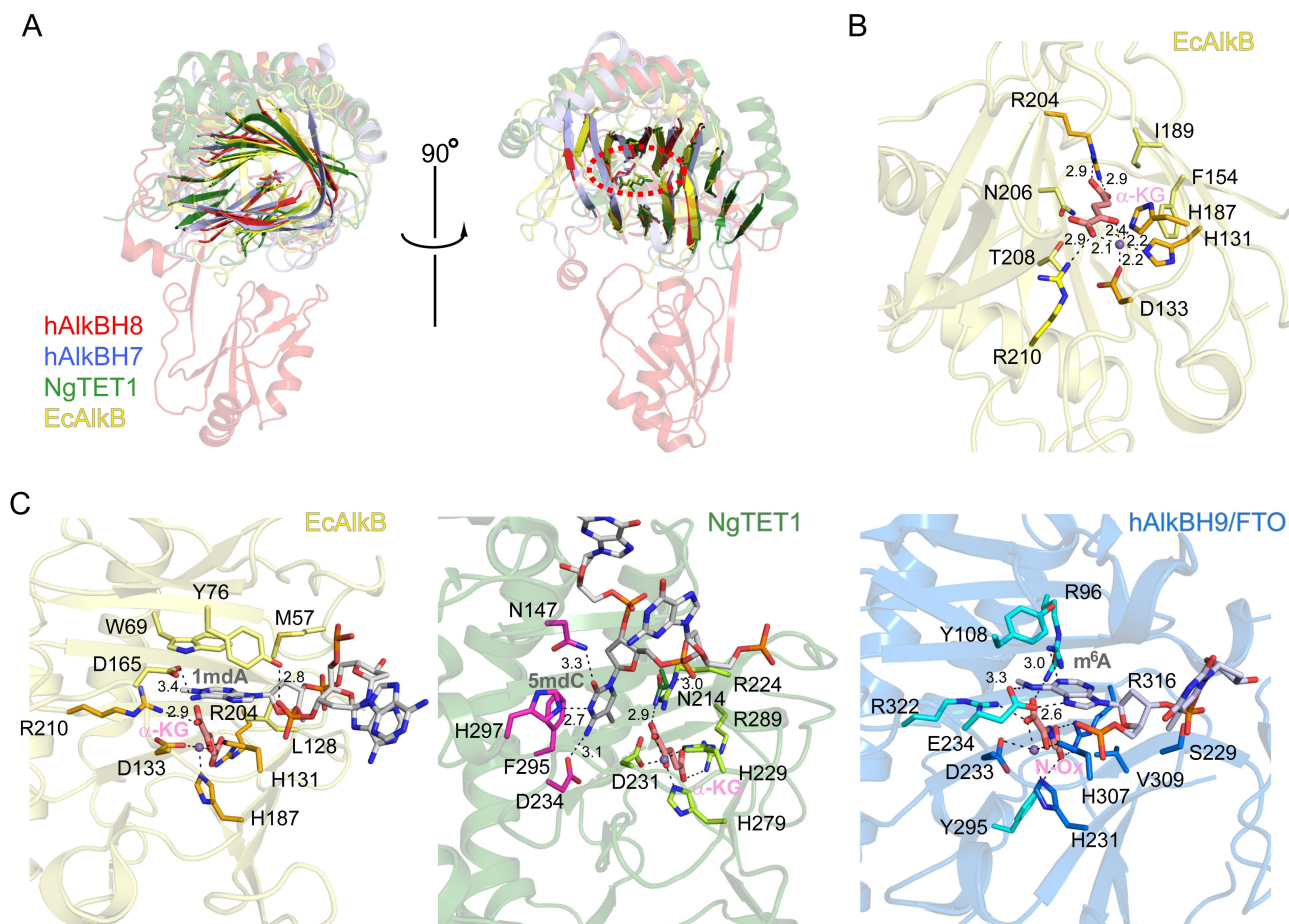


**Figure 2.** Structural comparison of  $\text{Fe}^{2+}/\alpha\text{-KG}$ -dependent enzymes. **A** Superposition of hAlkBH8 (red, PDB code 3THT, *Homo sapiens*), hAlkBH7 (blue, PDB code 4QKD, *Homo sapiens*), NgTET1 (green, PDB code 5CG9, amoeba *Naegleria gruberi*) and EcAlkB (yellow, PDB code 3BIE, *E. coli*) displayed as transparent ribbon, with the jelly-roll folding topology and  $\alpha\text{-KG}$  binding site highlighted.  $\alpha\text{-KG}$  is shown as stick-model. **B** Structure of the EcAlkB active site (PDB code 3BIE), with residues coordinating  $\text{Mn}^{2+}$  and  $\alpha\text{-KG}$  depicted as stick model. Amino acids coordinating  $\alpha\text{-KG}$  and the metal ion which are conserved across species are highlighted in golden. **C** Substrate recognition by NgTET1 (green, PDB code 5CG9), EcAlkB (yellow, PDB code 3BIE) and hAlkBH9 (blue, PDB code 5ZMD, *H. sapiens*) in complex with their respective substrates. Active site residues are depicted as stick models, with the residues involved in substrate and  $\alpha\text{-KG}/\text{N-Ox}$  recognition highlighted by color. Metal ions ( $\text{Mn}^{2+}$  or  $\text{Fe}^{2+}$ ) are drawn as purple spheres. Hydrogen bond distances are shown in Å. (N-Ox = N-oxalylglycine; 5mdC = 5-methyl deoxycytosine; 1mdA = *N*-methyl-deoxyadenine; *m*<sup>6</sup>A = *N*<sup>6</sup>-methyl-adenine).

substrate complexes (Figure 2C).<sup>[36g,37a,38b]</sup> All TET enzymes have the ability to catalyze the oxidation of 5mdC to 5hmdC, 5fdC and ultimately 5cadC in DNA. However, they exhibit not only differences in their large unstructured *N*-terminal domains, but also possess a distinct spatial-temporal cellular distribution during development and cellular differentiation.<sup>[47]</sup> In addition to the variability and flexibility of loops and domains in the different  $\text{Fe}^{2+}/\alpha\text{-KG}$ -dependent dioxygenases, which determine the substrate scope, alteration in active site dynamics through interaction with the cofactor  $\alpha\text{-KG}$  or byproduct succinate impacts on substrate binding and product release. NMR-spectroscopic analysis of EcAlkB revealed that the active site in the EcAlkB- $\text{Fe}^{2+}$ - $\alpha\text{-KG}$  complex is more rigid than the EcAlkB- $\text{Fe}^{2+}$ -succinate complex, indicated by an observable sharpening of the resonances and higher resolution spectrum.<sup>[48]</sup> In line with this observation, EcAlkB enters a catalytically competent folded state only when in complex with  $\text{Fe}^{2+}$  and  $\alpha\text{-KG}$ .<sup>[49]</sup> The use of NMR spectroscopy to gain more insight into the

dynamics of  $\text{Fe}^{2+}/\alpha\text{-KG}$ -dependent enzymes is described in more detail in the next section.

## 2.2. Structural and active site studies in solution

### 2.2.1. NMR spectroscopy

NMR spectroscopy has been widely utilized to investigate protein dynamics in the presence of substrates and cofactors. In general, proteins that are studied by NMR are smaller than ~30kDa, albeit due to recent technical advances data on larger monomeric proteins and protein complex have been reported. Here also the required isotope labelling of the protein in order to unambiguously assign NMR signals provides additional challenges for structure determination.<sup>[50]</sup> A study of EcAlkB dynamics and how the binding of cofactor  $\alpha\text{-KG}$  or the byproduct succinate is altered in the presence of substrate

which results in different dynamic properties of these complexes, was reported by Matthews and co-workers.<sup>[48]</sup> Initially, they found that between 0.5 and 1.5 ppm the EcAlkB–Fe– $\alpha$ -KG complex exhibited sharper resonances and better resolved NMR spectra than the EcAlkB–Fe–succinate counterpart (Figure 3). The same trend was observed with  $\text{Co}^{2+}$  as the central metal ion. The authors concluded that the  $\alpha$ -KG-bound form is more rigid than the succinate-bound form and this was proposed to be an important feature for effective product release.  $^1\text{H}$ – $^{15}\text{N}$ –HSQC was used for backbone assignment and proved useful in the case of the  $\alpha$ -KG-bound complex.  $^1\text{H}$ -spectrum pseudo-contact shifts verified the presence of high-spin  $\text{Fe}^{2+}$  in the active site. In contrast, some very broad, nearly undetectable peaks confirmed the increased dynamic motion of the

succinate-bound complex. Within the detected signals, 25 peaks with different shifts indicating different chemical environment were found (Figure 3, right).

Comparison of the shifted signals with the crystal structure revealed that the observed amino acids are all close to  $\alpha$ -KG. In the crystal structure, no channel for  $\alpha$ -KG/succinate exchange is observed, thus dynamic flexibility and conformational change upon  $\alpha$ -KG-succinate conversion is essential and allows for the efficient dissociation of the products. A follow-up study, already mentioned in section 2.1, by Bleijlevens, Matthews and co-workers confirmed that only with both  $\text{Fe}^{2+}$  and  $\alpha$ -KG bound to EcAlkB, the protein enters a catalytically competent folded state.<sup>[49]</sup> Figure 4A shows the sharp  $^1\text{H}$  resonances of holo-EcAlkB around  $-1$  ppm indicating a well-folded protein. The

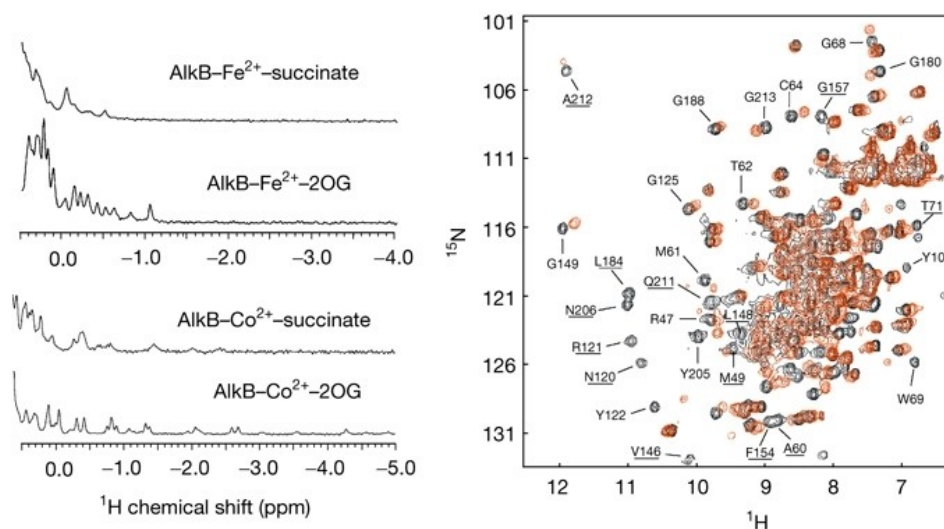


**Figure 3.** Copyright © 2008, European Molecular Biology Organization.<sup>[48]</sup> Left:  $^1\text{H}$  NMR of EcAlkB–Fe/Co complexes with either succinate or  $\alpha$ -KG bound. Right:  $^1\text{H}$ – $^{15}\text{N}$  HSQC of EcAlkB/Fe $^{2+}$ / $\alpha$ -KG (black) and EcAlkB/Fe $^{2+}$ /succinate (red).

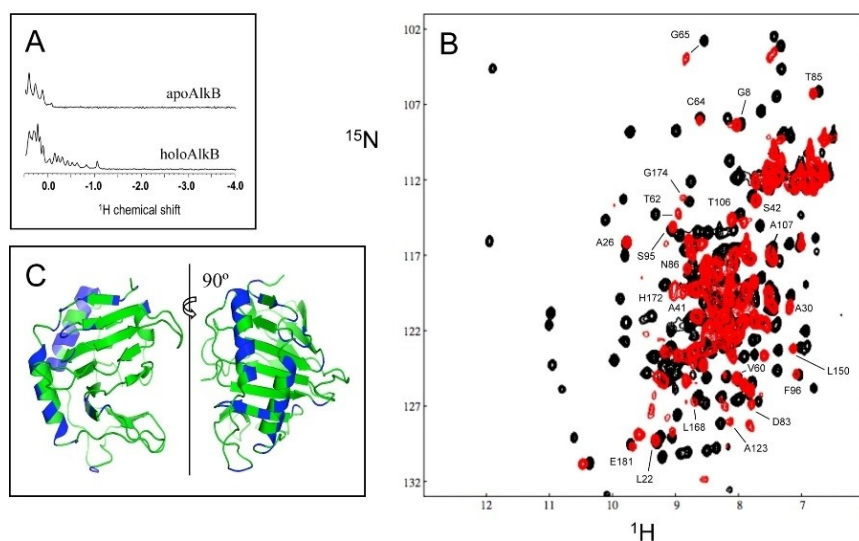


**Figure 4.** Copyright © 2012, American Chemical Society.<sup>[49]</sup> Changes of EcAlkB folding can be monitored by NMR. **A**  $^1\text{H}$  NMR spectra of apo-EcAlkB and holo-EcAlkB (EcAlkB/Fe $^{2+}$ / $\alpha$ -KG). **B**  $^1\text{H}$ – $^{15}\text{N}$  NMR spectra of apo-EcAlkB (red) and holo-EcAlkB (black). **C** Holo-EcAlkB (PDB 2FD8, active site and substrate omitted) with the position of tentatively assigned residues that are affected by cofactor binding highlighted in blue.



marked differences in folding between apo- and holo-EcAlkB became even more obvious in a  $^1\text{H}$ - $^{15}\text{N}$  NMR experiment (Figure 4B). The location of the residues mainly affected by  $\text{Fe}^{2+}$  and  $\alpha\text{-KG}$  binding are mapped in blue onto the ribbon diagram of the structure (Figure 4C).

In a complementary study, the Hunt group studied binding dynamics of [ $^{13}\text{C}$ ]-methionine-enriched EcAlkB to a DNA substrate in the presence of  $\text{Zn}^{2+}$  (to avoid paramagnetic shifting) and  $\alpha\text{-KG/succinate}$ .<sup>[51]</sup> While they propose that apo-EcAlkB adopts a defined conformation rather than a globule-like structure (termed 'open' conformation), their  $^1\text{H}$ ,  $^{13}\text{C}$  and  $^1\text{H}$ - $^{13}\text{C}$  correlation spectra indicate that addition of the co-factors modulates one distinct transition from the 'open' to a more rigid 'closed' conformation which also includes binding interaction with the DNA substrate. Not only  $\text{Fe}^{2+}$ ,  $\text{Co}^{2+}$  and  $\text{Zn}^{2+}$ , can be used to reconstitute EcAlkB, NMR spectroscopy also revealed a properly folded protein after  $\text{Cu}^{2+}$  binding.<sup>[52]</sup> This is particularly advantageous to study the distinct properties of the EcAlkB active site, when bound to  $\text{Cu}^{2+}$  using Electron Paramagnetic Resonance (EPR) spectroscopy.

### 2.2.2. EPR spectroscopy

EPR spectroscopy can be useful to gain insight into the changes in geometry and coordination sphere around the metal ion in the presence or absence of substrate and cofactors. In EPR, the effect of ligands on the central metals' unpaired electron(s) can be measured and used to deduce structural and electronic information. However, the native metal ion of the enzymes in question,  $\text{Fe}^{2+}$  ( $d^6$ , high spin), is very difficult to observe with this method due to it generating complicated spectra as a result of spin-orbit coupling as well as hyperfine coupling.<sup>[53]</sup> In addition, the allowed EPR transitions in  $\text{Fe}^{2+}$  ions occur at very high magnetic fields which typically lie outside the range of common spectrometers. Hence, researchers have substituted it for the excellent EPR probe  $\text{Cu}^{2+}$  to enable active site analysis of  $\text{Fe}^{2+}/\alpha\text{-KG}$ -dependent dioxygenases. Matthews *et al.* investigated the active site coordination environment in EcAlkB and classified the metal coordination site as a so-called type 2 copper site, i.e. the metal is bound by three to four amino acid residues of which at least one is His,<sup>[54]</sup> based on EPR data.<sup>[52]</sup> Although copper binding yields an inactive protein and this metal typically exhibits a lower coordination number than observed with ferrous ions, the authors showed *via* NMR and CD spectroscopy that the secondary and tertiary structure of EcAlkB with  $\text{Cu}^{2+}$  is identical to the native EcAlkB containing  $\text{Fe}^{2+}$ . Several different geometries<sup>[55]</sup> have been reported for copper centers bound to proteins such as octahedral or square pyramidal geometries that were observed in the crystal structure of the iron transporter lactoferrin binding  $\text{Co}^{2+}$  instead of  $\text{Fe}^{2+}$ .<sup>[56]</sup> Figure 5 shows the X-band EPR spectra of different EcAlkB- $\text{Cu}^{2+}$ -substrate combinations, recorded at 20 K. The EcAlkB- $\text{Cu}^{2+}$ - $\alpha\text{-KG}$  complex produced an axial spectrum ( $g_x = g_y = 2.06$ ) with parameters indicative of a type 2 copper site ( $g_z = 2.334$ ,  $A_z = 145$  G). Furthermore, following the work of Peisach and Blumberg, who derived correlation plots of

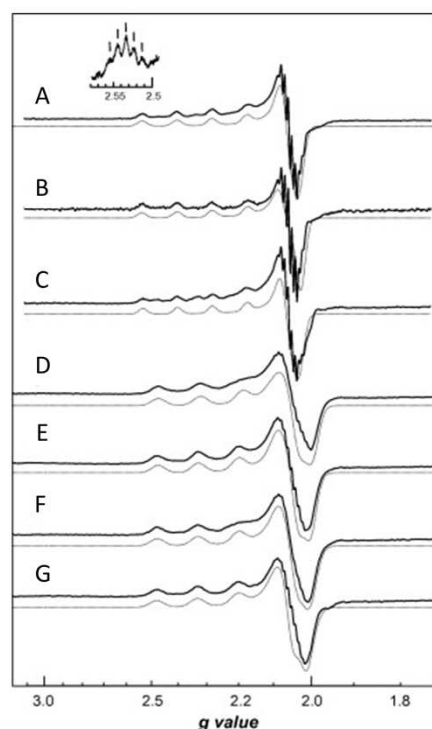


**Figure 5.** Copyright © 2007 Elsevier<sup>[52]</sup> A EcAlkB- $\text{Cu}^{2+}$ - $\alpha\text{-KG}$ , B EcAlkB- $\text{Cu}^{2+}$ - $\alpha\text{-KG}$ -imidazole, C EcAlkB- $\text{Cu}^{2+}$ - $\alpha\text{-KG}$ -meDNA, D EcAlkB- $\text{Cu}^{2+}$ , E EcAlkB- $\text{Cu}^{2+}$ -imidazole, F EcAlkB- $\text{Cu}^{2+}$ -succinate, G EcAlkB- $\text{Cu}^{2+}$ -succinate-imidazole. Solid lines correspond to recorded spectra and grey lines represent corresponding simulations. Conditions: 20 mM Tris-HCl, pH 7.6.

$g_z$  and  $A_z$  and grouped areas representing the varying oxygen and nitrogen coordination environments of the copper centers, the parameters of EcAlkB were shown to be characteristic for a mixture of oxygen and nitrogen donors.<sup>[52,57]</sup> Nitrogen coordination was further confirmed by the superhyperfine coupling pattern of the high field  $g_z$  line. Here, the five-line pattern (intensities 1:2:3:2:1) indicates a coupling to two  $I = 1$  nuclei ( $^{14}\text{N}$ ) in the  $xy$ -plane, consistent with coordination by two histidine residues in the active site. Interestingly, the addition of imidazole (Figure 5B), DNA (not shown) and methylated DNA (Figure 5C) to EcAlkB- $\text{Cu}^{2+}$ - $\alpha\text{-KG}$  complex did not result in notable changes in the spectra. Hence, substrate binding does not occur near the active site metal, consistent with X-ray structural data. However, when the cofactor  $\alpha\text{-KG}$  is absent or replaced by succinate, the active site gains enough flexibility and is able to bind imidazole. This example study demonstrates how EPR spectroscopy can yield structural and dynamic information about the interaction of active site residues with the substrates, albeit in frozen solution and with the replacement of the native metal ion by copper(II).

### 2.2.3. Fluorescence spectroscopy

Steady-state and time-resolved fluorescence can be used to examine changes in local protein dynamics and folding *via*

tryptophan reporters. EcAlkB contains four tryptophan residues which show a fluorescence maximum at 343 nm, with the fluorescence intensity depending on the micro environment, which can therefore be exploited for this purpose.

Addition of  $\text{Fe}^{2+}$  to EcAlkB causes quenching of the Trp-fluorescence, which is reduced even further when both  $\text{Fe}^{2+}$  and N-Ox (this inhibitor was used instead of  $\alpha$ -KG to avoid background activity of the enzyme) are added (Figure 6A).<sup>[49]</sup> This observation was attributed to an increased ordering of the holo-EcAlkB enzyme tertiary structure. Furthermore, the fluorescence anisotropy was largest when both  $\text{Fe}^{2+}$  and N-Ox were added (Figure 6B), reflecting lower mobility of the Trp-side chains. This finding also points to a decreased flexibility of the tryptophan-bearing domains in the fully assembled enzyme. Analogously, EcAlkB affinity towards other metal cations such as  $\text{Co}^{2+}$  and  $\text{Ni}^{2+}$ <sup>[58]</sup> as well as the conformational changes of the respective enzyme domain upon binding of  $\alpha$ -KG<sup>[51]</sup> were tracked and the fate of the nucleotide recognition lid when accommodating a DNA substrate was analyzed.<sup>[51,58]</sup> Trp-fluorescence is further amenable to investigate the thermal stability of these enzymes.<sup>[49]</sup> The behavior of EcAlkB apo-protein upon heating (Figure 6C) is perplexing because the fluorescence intensity decreases continuously with temperatures above 10 °C. This observation could indicate a higher stability of the protein complex which seemed to undergo a two-stage unfolding process. Yang, He and co-workers used these alterations in Trp-fluorescence to study the interaction of AlkBH2 with different substrates to probe how the enzyme senses base pair stability in duplex DNA.<sup>[30e]</sup> Information about the kinetics of (co-)substrate binding can be accessible through combining fluorescence spectroscopy, which works on a very small time scale, with the Stopped-Flow technique. This way, Fedorova *et al.* were able to propose a kinetic model for the conformational behavior of EcAlkB upon metal and DNA

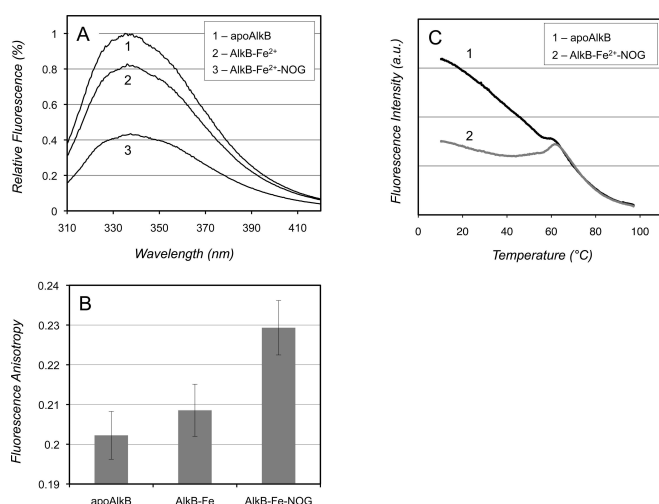


**Figure 6.** Copyright © 2012, American Chemical Society, taken from reference.<sup>[49]</sup> **A** Typical steady-state fluorescence of tryptophan residues in apo-EcAlkB and EcAlkB- $\text{Fe}^{2+}$  with (holo-EcAlkB) and without N-Ox. **B** Fluorescence anisotropy. **C** Thermal denaturation curves. Conditions: EcAlkB 7  $\mu\text{M}$ ,  $\text{Fe}^{2+}$  10  $\mu\text{M}$ , N-Ox 1 mM in 20 mM Tris-HCl, pH 7.6. EcAlkB 1  $\mu\text{M}$  in 20 mM Tris-HCl containing 150 mM NaCl, pH 7.6, 20 °C.

binding, based on the temporal course of the Trp fluorescence signal.<sup>[58]</sup> This spectroscopic approach has been extended to track the fluorescence of 2-aminopurine, which had been placed 3' to the 1mdA lesion to be repaired by EcAlkB in DNA, and to measure Förster Resonance Energy Transfer (FRET) when an oligonucleotide modified with a 5'-Fluorescein Amidite (FAM) fluorophore and a 3'-Black Hole Quencher 1 (BHQ1) quencher was employed.<sup>[59]</sup> This allowed for approaching EcAlkB protein dynamics from multiple angles.

Besides through mere quenching of fluorescence, the structural dynamics of a protein upon substrate binding can also be assessed *via* monitoring of the polarization of the emitted light.<sup>[60]</sup> While freely rotating fluorophores, such as a fluorescent label (fluorescein, carboxyfluorescein) at the 5'-end of a DNA strand in solution, commonly show barely polarized or non-polarized emission when excited with polarized light, restriction of rotational freedom through binding to a protein can result in retained polarization of fluorescence. This behavior is exploited in Fluorescence Anisotropy (FA) spectroscopy which has been applied in various studies of biomolecule interactions (and even live-cell imaging) and can provide information about structural, kinetic and thermodynamic properties of DNA-protein interaction when monomer and complex differ significantly in size. FA spectroscopy, in combination with point variant experiments, helped Holland and Hollis determine two different binding conformations ('searching' and 'repair') of EcAlkB when screening a DNA strand for methylation damage.<sup>[30a]</sup> Hunt and co-workers added evidence (through both FA and Trp-fluorescence quenching experiments) that EcAlkB preferentially binds alkylated DNA rather than non-alkylated DNA as a result of a conformational change from the 'open' to the 'closed' state induced by metal/co-substrate binding.<sup>[51]</sup> Apart from the generally very thoroughly studied EcAlkB enzyme, two of its human homologues were subjected to FA spectroscopy to elucidate their binding behavior towards their primary substrates. Multiple variants of AlkBH8, which usually act on modified uracil in some tRNAs, were provided with synthetic RNA strands and their binding affinities to those substrates appeared to be dependent on both the RNA recognition motif close to the N-terminus and an additional N-terminal  $\alpha$ -helix domain, even though with rather low sequence specificity.<sup>[35]</sup> Jia *et al.*, on the other hand, utilized FA spectroscopy in their structural study of AlkBH9 with its main substrate  $\text{m}^6\text{A}$  in mRNA, to screen for AlkBH9 variants suitable for crystallization which would exhibit increased binding affinity to 6mdA-containing DNA instead of RNA without significant impact on demethylation efficiency.<sup>[36g]</sup> They identified a Gln86Lys/Gln306Lys variant with 16-fold increased binding affinity compared to the wild type enzyme, which allowed for more facile crystallization and enabled them to structurally characterize the preference of AlkBH9 for binding of  $\text{m}^6\text{A}$  in the 5'-cap motif of mRNA. FAM-labelled DNA samples have been used to explore the binding affinity of 5mdC, 5hmdC, 5fdC or C-containing DNA and TET2. The fluorescence polarization measurements showed that the affinity for all four substrates was similar and was further unaffected by the presence of  $\text{Fe}^{2+}$ / $\text{Mn}^{2+}$  and N-Ox/ $\alpha$ -KG.<sup>[38b]</sup>

### 2.2.4. Isothermal titration calorimetry (ITC)

ITC is a method that can be used to monitor the thermodynamics of metal and substrate binding events to proteins as well as to obtain equilibrium constants and even kinetic information on substrate turnover.<sup>[61]</sup> In the previously mentioned study by Matthews and co-workers,<sup>[48]</sup> the binding affinity of EcAlkB to a DNA substrate at different stages of the oxidative catalytic cycle was assessed (Figure 7). Figure 7A shows the results for binding of methylated T(1mdA)T to EcAlkB–Fe<sup>2+</sup>– $\alpha$ -KG representing the situation at the pre-chemistry stage. After oxidative catalysis, the co-substrate has been oxidatively decarboxylated to succinate impacting on DNA binding which was modelled by titrating T(1mdA)T to EcAlkB–Fe<sup>2+</sup>–succinate (Figure 7B). The situation after oxidative demethylation of the DNA substrate was investigated with an unmethylated DNA pentamer binding to EcAlkB–Fe<sup>2+</sup>–succinate (Figure 7C). The authors had shown by NMR and CD spectroscopy (see Sections 2.2.1 and 2.2.5) that the succinate-containing holoenzyme exhibited higher conformational flexibility than the  $\alpha$ -KG-containing complex. This is also reflected by the ITC data, as the methylated trimer was bound more strongly by EcAlkB–Fe<sup>2+</sup>– $\alpha$ -KG than by EcAlkB–Fe<sup>2+</sup>–succinate. Notably, biphasic isotherms were obtained in both cases (discernable from the presence of a saddle point in the curves and the derivability of two  $K_d$  values from them). This was attributed to two different EcAlkB species of which one might have undergone auto-oxidation with a different affinity for substrate. Upon dealkylation of the substrate, the binding affinity to the now unmethylated DNA drops dramatically (as reflected in the higher  $K_d$  value in Figure 7C) hinting to further increased flexibility as a prerequisite for substrate release. It should be

noted, though, that the unmethylated substrate is of a different length and sequence (TTdCTT) than the substrate in the first two cases (T(1mdA)T), so that potential sequence biases were not accounted for.

The DNA binding properties of TET enzymes have also been tested by ITC. As the DNA-binding CXXC domain of TET enzymes lacks a sequence motif which determines the properties of other CXXC-containing enzymes,<sup>[62]</sup> Shi *et al.* examined the *Xenopus* TET3 CXXC domain (as well as the human version) *via* ITC.<sup>[39b]</sup> Indeed, while preferring CpG-containing sequences, TET3 CXXC also binds to non-CpG oligonucleotides with similar specificity as long as one dC or dG is present. This distinguishes it from, *e.g.*, CFP1 or MLL which exhibit strict dependence on CpG dinucleotides.<sup>[62]</sup> They further identified an unmodified cytosine as indispensable for TET3 CXXC binding.<sup>[39b]</sup> These ITC data provided a principle foundation for a subsequent analysis of the genome-wide TET3 CXXC binding profile (in HEK293T cells) by other, DNA sequencing-based, techniques, demonstrating that simplified *in vitro* assays can help elucidate biological observations. Isothermal Titration Calorimetry further showed that mammalian TET3 had high binding affinity to 5cadC compared to unmodified dC in a dC(xdC)dG context, while binding to 5mdC, 5hmdC and 5fdC was markedly reduced.<sup>[39a]</sup> ITC can even be useful in screening for (non-DNA) high-affinity inhibitors of such enzymes, as exemplified by Yu and co-workers who established a small-molecule inhibitor for TET2 which was consequently employed to investigate the role of TET2 in somatic cell reprogramming.<sup>[63]</sup>

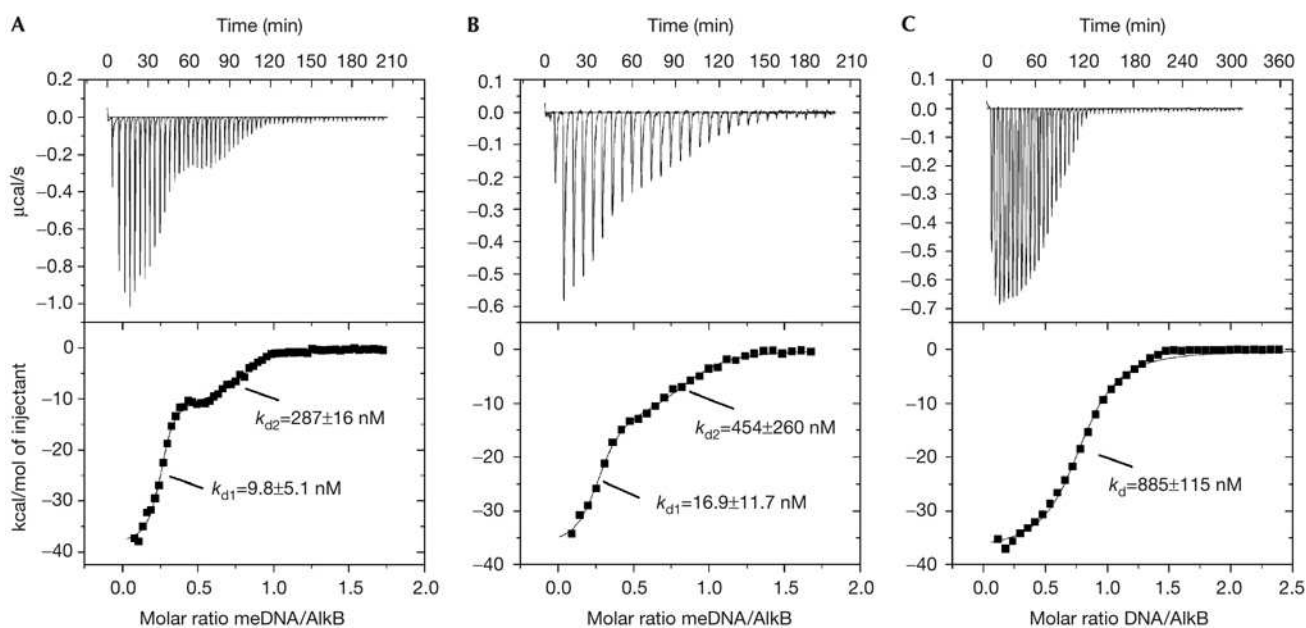


**Figure 7.** Copyright © 2008, European Molecular Biology Organization.<sup>[48]</sup> Isothermal calorimetric titrations (ITC), top: calorimetric titration profiles, bottom: fit of heat absorbed per mole of titrant versus DNA/EcAlkB ratio. **A** Binding of T(1mdA)T to EcAlkB–Fe<sup>2+</sup>– $\alpha$ -KG. **B** Binding of T(1mdA)T to EcAlkB–Fe<sup>2+</sup>–succinate. **C** Binding of unmethylated DNA (here: TTdCTT) to EcAlkB–Fe<sup>2+</sup>–succinate.<sup>[48]</sup>

### 2.2.5. CD spectroscopy

Circular Dichroism (CD) spectroscopy is an excellent method to determine correct folding of proteins and secondary structure traits, to investigate interactions of proteins with substrates and to monitor concomitant conformational changes as well as the impact of temperature, denaturants and additives.<sup>[64]</sup> Ideal for this method are inorganic buffer systems such as phosphate, but HEPES (2-[4-(2-hydroxyethyl)piperazin-1-yl]ethane-1-sulfonic acid) and Tris (tris(hydroxymethyl)aminomethane) have likewise been used successfully in CD spectroscopy. Matthews and co-workers reported the CD spectra of EcAlkB in the presence of  $\alpha$ -KG (here labelled as 2OG) and succinate.<sup>[48]</sup> To stabilize the native metal ion  $\text{Fe}^{2+}$ , ascorbate is usually included, however this additive possesses an intense CD signal in the near UV-region obscuring the EcAlkB signature. For an excellent discussion on the role of ascorbate for  $\alpha$ -KG/Fe-dependent oxygenases please see reference.<sup>[65]</sup> Due to the observed auto-oxidation of the EcAlkB- $\text{Fe}^{2+}$  species in the presence of  $\text{O}_2$ , metal ion substitution with  $\text{Co}^{2+}$  was consequently explored. Hunt *et al.* had previously demonstrated that the active site structures of  $\text{Fe}^{2+}$  and  $\text{Co}^{2+}$ -substituted EcAlkB are nearly

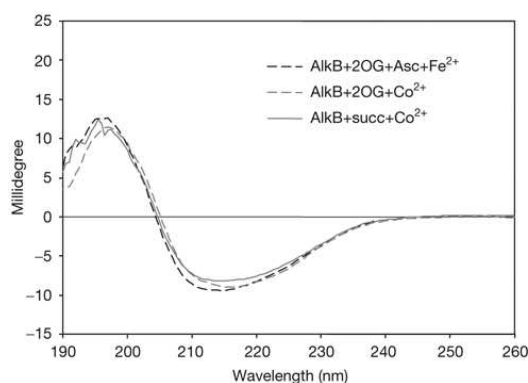


**Figure 8.** Copyright © 2008, European Molecular Biology Organization. CD spectra of EcAlkB in the presence of different cofactors and metal ions.<sup>[48]</sup> Conditions: 20 °C, 1 mm path length, 12.5  $\mu\text{M}$  EcAlkB, 1 mM Ascorbate, 1 mM Tris-HCl pH 7.6. Background signals from buffer and cofactors were subtracted from the spectra.

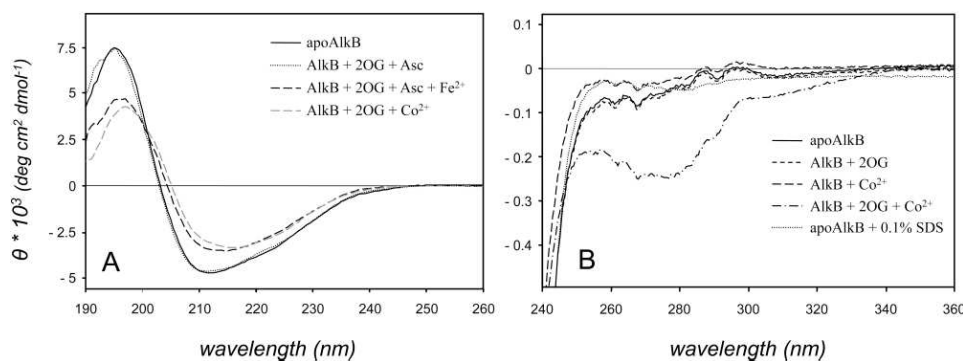


**Figure 9.** Copyright © 2012, American Chemical Society, taken from reference.<sup>[49]</sup> **A** Far-UV spectra and **B** Near-UV spectra. Conditions: Far-UV CD spectra = 1 mm path length quartz cuvette, 20 °C, 12.5  $\mu\text{M}$  EcAlkB (0.3 mg/mL) in 1 mM Tris-HCl, pH 7.6. Near-UV CD spectra = 4 mm path length quartz cuvette, 10 °C, 1 mg/mL EcAlkB in 20 mM Tris-HCl, pH 7.6. Spectra corrected for background signals.

identical, hence no major structural changes upon metal addition are expected.<sup>[30c]</sup> Besides  $\text{Co}^{2+}$ ,  $\text{Cu}^{2+}$  is also suitable for reconstitution of the active site without distinct changes in the secondary and tertiary structures, while yielding an inactive, but stable enzyme for structural investigations.<sup>[52]</sup> Spectral fitting of the CD spectra in Figure 8 showed that EcAlkB mostly consists of  $\beta$ -sheets (39%) and only  $< 10\%$   $\alpha$ -helices, and revealed that no significant structural changes upon  $\alpha$ -KG or succinate binding were induced.<sup>[48]</sup>

Several years later, the same group reported a comparison of apo-EcAlkB and holo-EcAlkB in the presence of different cofactors.<sup>[49]</sup> Consistent with previous reports, CD-spectroscopic analysis demonstrated predominant  $\beta$ -sheet contribution, in accordance with the structural motifs found in the crystal structure. Interestingly, both the maximum (195 nm) and minimum (210 nm) intensify upon metal binding, possibly because the metal binds to two residues that are part of a  $\beta$ -barrel and thus stabilize the structures. The nature of the metal (Fe, Co) had little influence and the addition of  $\alpha$ -KG did not alter the spectra significantly (Figure 9A). Absorbance in Near UV is commonly caused by disulfide bridges and aromatic residues. EcAlkB does not contain any disulfide bridges, however, aromatic residues are integrated into the protein structure in unique ways upon folding, hence, they can be used to probe a proteins tertiary structure. The spectrum of holo-EcAlkB is markedly different in the near-UV region, pointing towards variation between apo-EcAlkB and holo-EcAlkB tertiary structure (Figure 9B). Hunt *et al.* reported another study on the folding behavior of wild type and mutant EcAlkB variants dependent on the presence of viable co-factors.<sup>[51]</sup> Through following protein denaturation upon heating, thermodynamic stabilization of the holo-enzyme by ligand binding was observed, further supported by NMR and FA spectroscopy experiments.

At the time of writing, we were unaware that magnetic circular dichroism (MCD) or variable-temperature, variable-field (VTVH) MCD spectroscopy had been applied to any of the relevant enzymes discussed in this review. In particular, local modifications of the iron coordination site, such as changes in coordination number during cofactor and substrate binding,

can be elucidated with these methods.<sup>[66]</sup> A possible question that could be addressed with MCD would be how readily a catalytically competent active center is formed in the presence of a certain substrate, which in turn could help with assigning native functionality. In addition to CD and MCD spectroscopy, UV/Vis spectroscopy is widely utilized in the concerned area of research and some examples are given in the next paragraph.

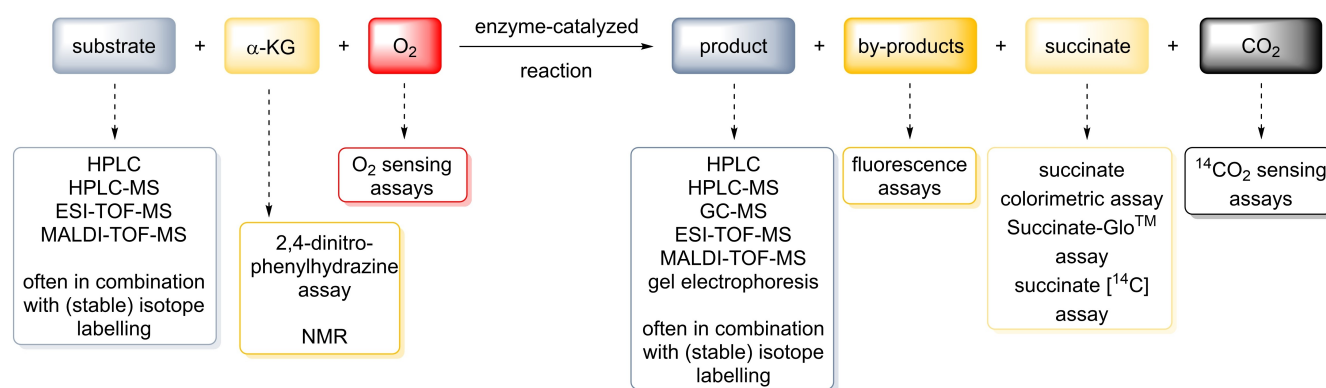
### 2.2.6. UV/Vis spectroscopy

UV/Vis absorption spectroscopy is, except for the spectroscopically silent metals  $\text{Cu}^+$  and  $\text{Zn}^{2+}$  (full d-shell,  $d^{10}$ ), widely used in bioinorganic chemistry to investigate the characteristic features of metalloproteins. In 2002 Sedgwick, Hausinger and co-workers confirmed for the first time experimentally that EcAlkB is an  $\text{Fe}^{2+}/\alpha\text{-KG}$ -dependent enzyme, partly based on the observation of a weak Metal-to-Ligand-Charge-Transfer (MLCT) band around 500 nm, reflecting charge transfer from  $\text{Fe}^{2+}$  to  $\alpha\text{-KG}$ .<sup>[20d]</sup> This type of MLCT is a characteristic feature of  $\text{Fe}^{2+}/\alpha\text{-KG}$ -dependent dioxygenases.<sup>[4]</sup> The authors compared the difference spectra of anaerobic apo-EcAlkB with  $\alpha\text{-KG}$  in the presence and absence of iron and also noted that the absorption maximum of 500 nm was slightly shifted compared to other members of the  $\text{Fe}^{2+}/\alpha\text{-KG}$  enzyme family (530 nm).<sup>[20d]</sup> Previously reported UV/Vis signatures of EcAlkB were at  $\lambda_{\text{max}} = 560 \text{ nm}$ <sup>[67]</sup> or described as broad band around 450–500 nm.<sup>[20d]</sup> The difference in absorption maxima was attributed on whether iron was already present from purification or added to the purified apo-enzyme.<sup>[67]</sup> Once oxygen is introduced into these systems (in the absence of substrate), self-hydroxylation of the enzymes can be observed (also referred to as uncoupled decarboxylation). In TauD and EcAlkB this is reflected by a band around 550 nm (oxidation of a tyrosine residue)<sup>[68]</sup> and 595 nm (tryptophan oxidation),<sup>[69]</sup> respectively. These spectral changes are most likely due to Ligand-to-Metal-Charge-Transfer (LMCT) from  $\text{Trp-OH}$  to  $\text{Fe}^{3+}$ .<sup>[70]</sup> This unwanted self-hydroxylation can be avoided by handling the enzyme under strictly anaerobic conditions, especially in the absence of a suitable substrate. For EcAlkB UV/Vis absorption spectroscopy was also used to

examine substrate binding and/or the ability to form a catalytically competent active center. Mishina, Chen and He investigated the impact of ssDNA binding on EcAlkB.<sup>[67]</sup> They observed that the  $\text{Fe}^{2+}$ - $\alpha\text{-KG}$  MLCT band at 560 nm broadened and shifted to 551 nm upon addition of ssDNA and attributed this to a geometry change around the iron center upon substrate binding. For TET2 the absorbance decay of the  $\text{Fe}^{\text{IV}}$ -oxido species was monitored in the presence of different substrates with stopped flow absorption spectroscopy. For this, an anaerobic solution of TET2 and  $\text{Fe}(\text{NH}_4)_2(\text{SO}_4)_2$  was mixed rapidly with a solution (that had been previously exposed to air and hence contained  $\text{O}_2$ ) of  $\alpha\text{-KG}$  and dsDNA bearing either 5mdC, 5hmdC or 5fdC. The emergence and decay of species VI (see Scheme 3, Figure 10) was then monitored at 318 nm. For 5hmdC and 5fdC containing substrates, the intensity of the signal in the beginning was larger than for 5mdC. Thus, the catalytically active  $\text{Fe}^{\text{IV}}$ -oxido species (species VI) accumulated when 5hmdC or 5fdC were present, before it was consumed by reaction with the substrate. The decay of this species was also slower for those two substrates than for 5mdC. The authors concluded that the substrate influences the reaction time and that the substrate preference in TET2 is caused not by altering the formation of the  $\text{Fe}^{\text{IV}}$ -oxido species but acts through the changes in the hydrogen abstraction step, which is the rate determining step.<sup>[38b]</sup>

### 2.2.7. Surface plasmon resonance (SPR) spectroscopy

Albeit surface plasmon resonance (SPR) spectroscopy (Biacore) has to our knowledge so far not been reported to be used for the characterization of AlkB-family oxygenases, SPR spectroscopy allows the *in situ* real-time and label-free detection of biomolecular interactions, which could be utilized for their functional investigation. Here the target molecule (i.e. protein or nucleic acid fragment) is immobilized on a prepared gold sensor surface and a solution with the potential interaction partner is applied through flow cells. Alteration of the mass on the sensor surface impacts on the intensity of the reflected, incident polarized light beam at a specific angle (=resonance



**Scheme 3.** Different possibilities to monitor activity of  $\text{Fe}^{2+}/\alpha\text{-KG}$ -dependent enzymes. “Substrate” here refers only to the nucleic acid substrate, not  $\alpha\text{-KG}$  or  $\text{O}_2$ . Similarly, “product” refers only to the nucleic acid product. Any other products are considered “byproducts”.

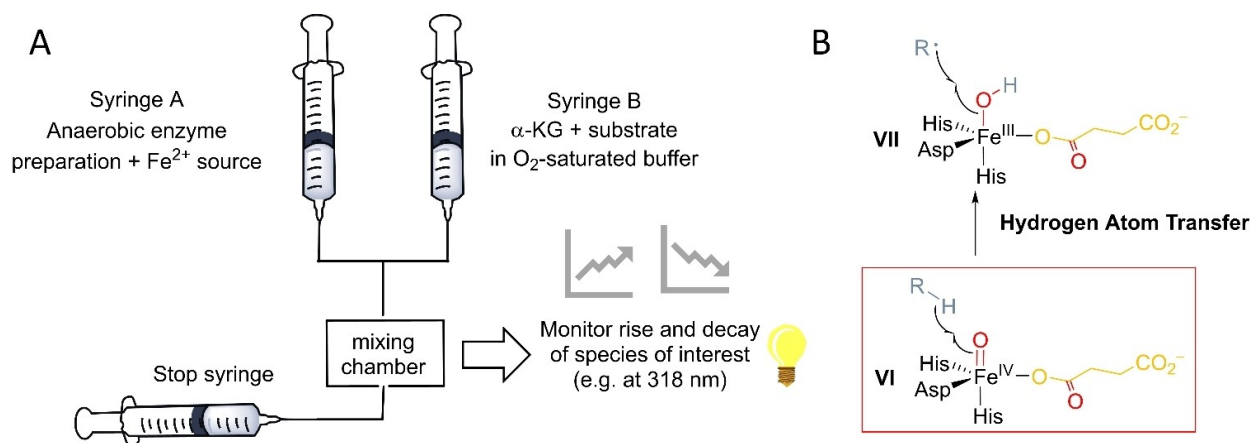


**Figure 10.** Stopped-flow with UV-Vis detection can be used to gain information how different substrates affect the formation and consumption of reactive species. A. Example of stopped flow setup. B. Formation of species VI as well as its decay can be monitored with stopped flow. In the case of TET2, it was reported that with 5mdC-containing DNA the decay was faster than for 5hmdC or 5fdC containing DNA, but the emergence of species VI was similar for all three. Thus, the hydrogen atom transfer step is likely the one that causes the observed substrate preference in TET2.

angle), from which information about binding affinity, dissociation and association rate constants and thermodynamic parameters, such as entropy, enthalpy, and activation energy can be deduced.<sup>[71]</sup> Luo, Hu and co-workers used this technique to assess the interaction of TET2 with 5mdC-, 5hmdC- and 5fdC-containing DNA.<sup>[38b]</sup> The authors used biotinylated DNA (26 base pairs including the cytosine modification of interest) that was immobilized on a streptavidin-chip to monitor the kinetics of association and dissociation of TET2 to the three DNA substrates. Since no significant differences were observed, they concluded that the DNA-binding affinity to TET2 is comparable between the substrates and that this is not the source of substrate preference for 5mdC-containing DNA.

### 3. Kinetic Investigations using Different Assay Methods

Over the past decades multiple assays have been developed that give insight into the kinetics and substrate turnover of Fe<sup>2+</sup>/α-KG-dependent enzymes that play a role in epigenetics and DNA repair, based on measurements of substrates and products of the enzymatic reaction. For nucleic acid substrates, the utilization of substrates and generation of products can be directly monitored by HPLC and different mass spectrometry (MS) methods (Scheme 3). Oxygen consumption can likewise be followed as well as the formation of CO<sub>2</sub> byproduct after the active species has been generated. Popular assays also rely on the emergence of succinate as byproduct of the C–H activation reaction and thus provide an indirect analysis of substrate turnover. For those enzymes eliminating alkyl groups from their substrates, the small molecules which are released might serve as activity indicators as well. Typically, combinations of these approaches are employed to obtain a broad image of enzyme

activity. In the following text, the different methods are critically discussed.

#### 3.1. Direct analysis of enzyme-specific substrates and products

A common practice for the study of enzymes is the analysis of the substrate or product after enzymatic treatment by a variety of techniques. In particular liquid, but also gas chromatography (both stand-alone and coupled with mass spectrometry) are widely used methods to determine substrate consumption and/or product formation. GC or HPLC and GC- or HPLC-MS analysis allow for the investigation of both *in vitro* and *in vivo* systems, if the samples are prepared accordingly.<sup>[22b,72]</sup> Various excellent descriptions of analytical procedures can be found in the literature.

For example, HPLC analysis of reaction products using isotopically labelled substrates in combination with measuring of the radioactivity in the sample can be used to track the demethylation activity of EcAlkB or related enzymes. Here, the methyl (or more general alkyl) group on oligonucleotides is [<sup>14</sup>C]-labelled and the radioactive activity in the supernatant analyzed by scintillation counting, giving detailed information on the activity of the studied enzymes. In 2003 Hausinger, Sedgwick and co-workers applied this combined procedure to show for the first time that EcAlkB demethylates 1mdA and 3mdC in DNA directly to dA and dC.<sup>[20d]</sup> They used the potent methylating agent [<sup>14</sup>C]-methyl iodide to methylate oligonucleotides (poly(dA) and poly(dC)) in combination with wt-EcAlkB or some EcAlkB variants. Following the enzymatic reaction, the nucleobases were digested and analyzed by HPLC, and the radioactivity in the supernatant determined by scintillation counting of the collected fractions. This was complemented by measuring the radioactivity of the ethanolic supernatants containing the eliminated formaldehyde. The study found that,

while 3mdA and 7mdA had also formed, they were not demethylated by EcAlkB. In a similar way, Krokan *et al.* tracked the fate of [<sup>3</sup>H]-methylated DNA and RNA substrates to study EcAlkB, hAlkBH2 and hAlkBH3.<sup>[22b]</sup> However, they focused their experiments on the detection of nucleosides and concluded, among others, that hAlkBH2 is more active on dsDNA than on ssDNA and that EcAlkB is involved in RNA repair. Kizaki and Sugiyama used HPLC to study TET activity on a hexameric substrate comprising only guanine, cytosine and 5mdC. They reported that, under *in vitro* conditions (55.4 μM CGmCGCG; 7.29 μM mTET1 active domain 1376–2039; 37 °C; 40 min) 5mdC is quickly converted to 5hmdC, already reaching its maximum level after only a few minutes incubation time. 5hmdC is further transformed to 5fdC, which reaches steady levels in a dynamic equilibrium after 10 min incubation, as it is continuously produced from 5hmdC, but also consumed to form 5cadC.<sup>[72a]</sup>

Currently, mostly MS-based techniques are applied, as the instruments are sensitive (detection limits down to a low femtomole range) and allow to detect epigenetic modified bases in a nucleic acid sample directly. For example, in 2019 Carell *et al.* published a protocol on the quantification of non-canonical natural DNA nucleosides, where they describe a short (14 min/sample) method in which DNA is extracted and digested, the sample diluted with isotopically labeled internal standards (<sup>13</sup>C and/or <sup>15</sup>N) that have similar chromatographic and fragmentation properties, followed by LC-MS quantification of the nucleosides.<sup>[73]</sup> By now this method has been adapted and used by several groups, for instance to determine the influence of epigenetics on cancer or to generally study the turnover of genomic methylcytosine in pluripotent cells.<sup>[72b,74]</sup> This method has also been used to detect levels of 5mdC, 5fdC and 5cadC after oxidation of a 5mdC containing oligomer by a TET biomimetic.<sup>[75]</sup> An excellent review was published on the detection, structure and function of modified DNA bases by Balasubramanian *et al.* in 2019, which dives into this topic in greater detail.<sup>[76]</sup>

In addition to HPLC analysis, gas chromatography has been utilized for the detection of DNA fragments. In 2015, Sowers *et al.* used a combination of HPLC separation and GC-MS analysis (detection limit also in the low femtomole range) to determine the amounts of cytosine modifications (probably as a result of TET activity) in rodent brain cells.<sup>[77]</sup> While HPLC(-MS) can be used to detect both nucleoside and nucleobase substrates, GC-MS requires the digestion of DNA to the nucleobases since (derivatized) nucleosides are not stable under the conditions of GC-MS. Derivatization of nucleobases with for example *N,O*-bis(trimethylsilyl)trifluoroacetamide (BSTFA) in acetonitrile and subsequent detection as well as quantification has been reported for a range of epigenetically relevant cytosine derivatives as well as for artificial DNA bases.<sup>[78]</sup>

Not only single nucleosides or nucleobases can be processed with HPLC, DNA oligomers can also serve as analytes. In 2009, Yu and Hunt published their results on EcAlkB activity on trimeric (TmdCT or TmdAT or TεdAT) or pentameric (3mdC or 1mdA in different combinations with C/T/A, as well as 1mdG, 3mT and εA) substrates.<sup>[79]</sup> They found that 3mdC and 1mdA lesions were repaired three orders of magnitude faster than εA

in the trimer, whereas repair activity on 1mdG and 3mT was decreased 10.000-fold compared to 1mdA or 3mdC. Similarly, Maciejewska and co-workers performed another in-detail study of EcAlkB activity on different randomly methylated pentamers containing 3mdC, εdA, εdC, hydroxyethyl C (HEC), or hydroxypropyl C (HPC).<sup>[20g]</sup> In an HPLC-based assay, they optimized the pH as well as the Fe<sup>2+</sup> and α-KG concentrations and calculated the rate constants for repair efficiency for each of these substrates. The authors observed the pH optimum for oxidation to consistently be one unit below the *pK<sub>a</sub>* of the substrate in all cases, indicating that cationic protonated substrates are preferred. Interestingly, the Fe<sup>2+</sup> dependence was found to be inversely correlated to the pH, with higher optimum Fe<sup>2+</sup> concentration at lower pH values. In contrast, no significant dependence for the α-KG concentration was detected.

In addition to chromatographic separation and subsequent quantification of substrates and reaction products, stand-alone MS analysis played a critical role in assessing enzyme activity.<sup>[20f,80]</sup> Essigmann *et al.* used a variety of MS methods (MALDI-TOF-MS, ESI-TOF-MS or Q-TOF-MS) without prior digestion to elucidate the scope of nucleic acid lesions that can be removed by EcAlkB *in vitro* as well as the kinetics of the repair reactions. By tracking the −4 charge state of an 16mer ssDNA oligonucleotide, they identified a variety of modifications EcAlkB is able to act upon, which include, among others, 1mdA, etheno-A, 6mdA (with an intermediate described in EcAlkB hydroxylation studies for the first time), 2mdG, 2etdG, furyl-G, THF-G, “α-hydroxypropanyl”-G, “γ-hydroxypropanyl”-G and “malonyl”-G (Scheme 2). These mainly toxicologically interesting alkylated nucleobases either are lesions found to be formed in the presence of metabolic side products and external chemicals, or served as substrate models for more complex lesions found *in vivo* (especially furyl-G and THF-G). Moreover, they were able to observe some intermediates of the repair mechanism and corroborated parts of their findings *via* GC-MS experiments.

Moreover, upon incubation of hAlkBH1 with oligomeric DNA substrates and subsequent analysis of the reaction products by gel electrophoresis by Hausinger and co-workers, revealed that hAlkBH1 is also able to cleave non-methylated DNA oligomers.<sup>[81]</sup> The authors found that this AP-lyase activity is neither dependent on Fe<sup>2+</sup> nor α-KG, nor serves ascorbate as an activator as had been observed for the demethylation activity of hAlkBH1.<sup>[21h]</sup> In addition, ssDNA-cleavage by AlkBH1 was also found to be unaffected by the presence of EDTA, Mg<sup>2+</sup>, Mn<sup>2+</sup> or Zn<sup>2+</sup> and by incorporating THF as an abasic-site analogue into their substrates, Hausinger and team were able to show that hAlkBH1 cleaved the 3'-position of abasic sites.<sup>[81]</sup> Cleavage of specific DNA sequences by restriction enzymes and glycosylases followed by gel-electrophoretic analysis can be a useful low-effort tool to investigate enzymatic modification of nucleobases. The main requirement is, however, that such a DNA-cleaving protein (as described above for hAlkBH1, this can also be the examined enzyme itself) is available which is able to hydrolyze a DNA strand in the presence of either the substrate or product base of the enzyme in question. For example, a *Bacillus subtilis* alkyl adenine DNA glycosylase was used by O'Brien *et al.* to study EcAlkB kinetics on 1mdA and εdA which

are both excised by the glycosylase initiating a DNA strand break under basic conditions.<sup>[82]</sup> Analysis of the fragmented and unfragmented oligonucleotides (carrying a fluorescent marker) on a gel allowed for a simple read-out of EcAlkB activity. It should be noted that they found rapidly decreasing instantaneous reaction rates in their steady-state kinetic assays which they attributed to potential self-inactivation of EcAlkB upon DNA binding. This might originate from self-hydroxylation at Trp178 and might be a potential cause for variable and inaccurate (hence not reproducible) kinetic parameters dependent on the time-scale of the measurement. To prevent this, the authors also performed steady-state experiments with 1mdA and  $\epsilon$ dA-containing DNA fragments in direct competition to each other, as well as single-turnover experiments. However, these approaches do not provide the same information as conventional steady-state kinetic assays and should rather be seen as complementary experiments.

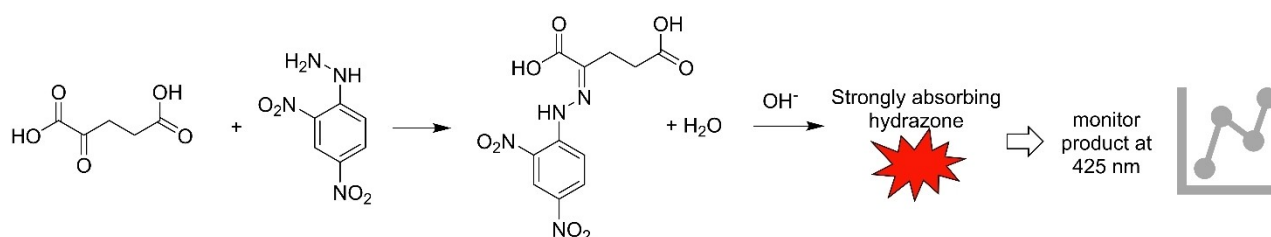
### 3.2. Direct analysis of co-substrates and byproducts

Besides relying on the detection of the nucleic acid substrates or products, a variety of approaches are available which exploit the conversion of the co-substrates,  $\alpha$ -KG and  $O_2$ , to the co-products succinate and carbon dioxide, specific substrate-independent hallmarks of the  $Fe^{2+}/\alpha$ -KG-dependent dioxygenase catalyzed reactions. Moreover, the AlkB dealkylase families produce further co-products, primarily formaldehyde or its homologues. Hence, this class of enzymes provides a diverse number of targets for activity studies, which are often combined to give a full picture of the enzymatic properties. Although the fates of  $\alpha$ -KG or its oxidation products are commonly tracked when investigating  $Fe^{2+}/\alpha$ -KG-dependent dioxygenases, such as deacetoxycephalosporin C synthase, prolyl hydroxylase and TauD,<sup>[83]</sup> the AlkB- and TET family enzymes have not been analyzed in detail *via* one of these strategies so far. Indeed,  $\alpha$ -KG has not yet been a considerable factor of interest in kinetic studies, although  $\alpha$ -KG turnover (or succinate formation) can be easily monitored with  $^1H$ -NMR spectroscopy.<sup>[84]</sup> Nevertheless, the formation of either carbon dioxide or succinate has been followed in a series of assays. In both cases, quantitative radioactivity measurements are typically undertaken after supplementing a mixture of approximately 10% [ $^{14}C$ ]-labelled  $\alpha$ -KG in unlabeled  $\alpha$ -KG. Isotopic labelling of the 1-carbon enables  $^{14}CO_2$  production

monitoring<sup>[83b]</sup> (after capturing with hydroxides), whereas 5- [ $^{14}C$ ]- $\alpha$ -KG application allows for observation of 1- [ $^{14}C$ ]-succinate.<sup>[85]</sup> It is noteworthy, however, that a recent study has found that  $\alpha$ -KG can, albeit slowly, be decarboxylated non-enzymatically in the presence of anti-oxidants like ascorbate or dithiothreitol, which are commonly used in activity studies of  $Fe^{2+}/\alpha$ -KG-dependent (di)oxygenses.<sup>[86]</sup> This was attributed to the formation of hydrogen peroxide from the anti-oxidant and dioxygen, which might then mediate  $\alpha$ -KG decarboxylation. In light of this, it might be worth performing assays tracking succinate or  $CO_2$  formation with additional controls, especially when high concentrations of anti-oxidant or long reaction times (*e.g.*, for inhibition studies or for investigation of variants with reduced activity) are required, to ensure the robustness of the acquired data. Unrelated to ascorbate/dithiothreitol, but along the line of commonly added (anti-oxidant) additives that may interact with metalloenzymes, Rodríguez-Maciá, Birrell and team have recently shown that for hydrogenases, the addition of the often-used reductant sodium dithionite influences the mechanism and thus spectroscopic features of this iron enzyme.<sup>[87]</sup> However, it should be noted that for the  $Fe^{2+}/\alpha$ -KG-dependent oxygenase TfdA (2,4-dichlorophenoxyacetate/ $\alpha$ -KG dioxygenase) it was reported that addition of dithionite remediated the effects of self-hydroxylation to some extent.<sup>[70]</sup> Recently, Haigis and co-workers have established a colorimetric  $\alpha$ -KG detection assay for the prolyl hydroxylases domain protein family.<sup>[88]</sup> The  $\alpha$ -KG consumption assay, relying on the derivatization of  $\alpha$ -KG with 2,4-dinitrophenylhydrazine (2,4-DNPH, Scheme 5) in the presence of concentrated base (Scheme 4), could also find use for the enzymes described in Table 1. Succinate does not form the colored product. However, it should be considered that 2,4-DNPH might react with formaldehyde, which can be a reaction product by AlkB-family dioxygenases (*e.g.* from 6mA demethylation).

#### 3.2.1. Carbon dioxide production assays

Based on  $^{14}CO_2$  quantification, hAlkBH1 was described as a histone demethylase, which regulates the methylation status of histone H2A, by Larsen and co-workers.<sup>[21a]</sup> Pollard *et al.* assessed the activity of hAlkBH5 towards a variety of methylated ssDNA substrates by this technique.<sup>[89]</sup> They first confirmed that hAlkBH5 is a  $Fe^{2+}/\alpha$ -KG-dependent dioxygenase by identifying one of their characteristic activity features: the so-



**Scheme 4.** Assay based on capturing  $\alpha$ -KG with 2,4-DNPH and subsequent treatment with base to yield a colored hydrazone product which can be quantified using UV-Vis absorption spectroscopy.



called uncoupled decarboxylation reaction,<sup>[90]</sup> which describes the oxidation of  $\alpha$ -KG followed by elimination of  $\text{CO}_2$  in the absence of a substrate. This reaction was found to be dependent on the presence of  $\text{Fe}^{2+}$  and the cofactor ascorbate, as expected for a  $\text{Fe}^{2+}/\alpha$ -KG-dependent dioxygenase.<sup>[89]</sup> Analogously, the  $\text{Fe}^{2+}$  and ascorbate dependent decarboxylation activity of hAlkBH1 was demonstrated by Krokan *et al.*<sup>[21h]</sup> Pollard and team further measured  $^{14}\text{CO}_2$  production to gain information on the dioxygen dependence of the hAlkBH5 uncoupled decarboxylation, which is strongly impaired under anaerobic conditions.<sup>[89]</sup> They linked this *in vitro* behavior to the upregulation of hAlkBH5 under hypoxia *in vivo* and proposed a specific function for AlkBH5 in hypoxic cells. However, no significant increase in  $\text{CO}_2$  production in the presence of methylated oligonucleotide substrates was found and the authors concluded that hAlkBH5 does not function as DNA demethylase.<sup>[89]</sup>

Other family-members whose activity was examined by analyzing the  $^{14}\text{CO}_2$  capture method were AlkBH2 and AlkBH3 (for their functionality in substrate recognition)<sup>[91]</sup> and the three TET proteins.<sup>[92]</sup>

### 3.2.2. Succinate production assays

In 1990, an activity assay based on the formation of 1- $^{14}\text{C}$ -succinate was developed by Kaule and Günzler for the investigation of prolyl 4-hydroxylase, which applies to any kind of  $\text{Fe}^{2+}/\alpha$ -KG-dependent dioxygenase.<sup>[85a]</sup> Since the radioactively labelled oxidation co-product is not volatile, capture is not required and it can be quantified *via* scintillation counting. However, unreacted 5- $^{14}\text{C}$ - $\alpha$ -KG must be removed beforehand, for instance, through precipitation as a hydrazone.<sup>[83a,93]</sup> This methodology was used to investigate several viral AlkB homologues which show activity against methylated nucleobases, especially in RNA context.<sup>[93]</sup> Krokan and co-workers reported hAlkBH1 to act on methylated adenines and cytosines in both mitochondrial DNA and RNA.<sup>[21h]</sup> Further, a lack of succinate release, in combination with other methods, implicated a lack of DNA demethylase activity in the case of a yeast AlkBH1<sup>[94]</sup> (even though it showed weak DNA lyase activity as found for hAlkBH1 by Hausinger *et al.*<sup>[81]</sup>). Analogous to the  $^{14}\text{CO}_2$  assay, 1- $^{14}\text{C}$ -succinate accumulation can be utilized to detect uncoupled decarboxylation. This approach was chosen by Andersson *et al.*, who investigated the general activity of AlkBH4, the substrate of which has not yet been identified.<sup>[95]</sup> Besides, different succinate-sensing strategies are (commercially) available, including colorimetric, coupled enzymatic assays.<sup>[83d,96]</sup>

### 3.2.3. Dioxygen consumption assays

Molecular oxygen is the second essential co-substrate of  $\text{Fe}^{2+}/\alpha$ -KG-dependent dioxygenases. Consequently, oxygen levels have been shown to modulate TET reactivity in tissues and hypoxia is known as an important factor in epigenetic

regulation and disease.<sup>[97]</sup> Surprisingly,  $\text{O}_2$ -levels in assays of epigenetically relevant enzymes are rarely controlled nor monitored *in vitro*, but have been reported for other  $\text{Fe}^{2+}/\alpha$ -KG-dependent enzymes and related non-heme enzymes (for example, by monitoring the decrease of atmospheric dioxygen levels).<sup>[66b,98]</sup> Depending on the assay design, this is likely to be due either to the necessity to initially prepare the reaction mixture under strictly oxygen-free conditions, or because the concentration is difficult to control without specialized equipment (e.g. oxygen electrode). For example, Sedgwich, Hausinger *et al.* monitored the consumption of oxygen by EcAlkB in the presence of 1mdA- or 3mdC-containing DNA-substrates potentiometrically, when they first characterized the enzyme's mode of action in detail.<sup>[20d]</sup> Using a Clark-type electrode<sup>[99]</sup> as an oxygen sensor, they showed that EcAlkB uses up significant amounts of dioxygen, if a suitable substrate is available, and that these amounts are stoichiometrically related to substrate oxidation. Since availability of dioxygen impacts on the activity of  $\text{Fe}^{2+}/\alpha$ -KG-dependent dioxygenases both *in vitro* and *in vivo*, these enzymes are commonly referred to as "physiological oxygen sensors" and contribute to metabolic changes under hypoxia.<sup>[100]</sup> Proteins as tightly connected to epigenetic processes as AlkB and TET family enzymes might be critical players in the cellular response to hypoxia as well as in disease and cancer development. The diminishing activity of hAlkBH5 with decreasing dioxygen concentration *in vitro*, demonstrated by Pollard and co-workers, and its consequent upregulation under such conditions *in vivo* provide some evidence for this connection.<sup>[89]</sup> TET1 and TET2 kinetics were measured more thoroughly with respect to  $\text{O}_2$  availability by Koivunen *et al.*<sup>[92]</sup> Here Michaelis-Menten analysis revealed a  $K_M$  around 30  $\mu\text{M}$  in both cases. In contrast, for the proline-4-hydroxylases which modify the hypoxia-inducible transcription factors (HIF-P4Hs) and initiate the cellular hypoxia response through being inhibited at dropping oxygen levels, a  $K_M = 230\text{--}250 \mu\text{M}$  was reported.<sup>[101]</sup> Thus, it was concluded that TET enzymes remain active even under hypoxic stress.<sup>[92]</sup> However, additional comparable studies providing detailed insight into those enzymes' behavior during dioxygen deficiency are required.

A remarkable, very different oxygen-sensing approach to measuring TET2 kinetics was developed by Dai, Zhang and co-workers in 2018, which is based on the luminescence of a  $\text{Cu}^+$ -containing metal-organic framework (MOF, Figure 11).<sup>[102]</sup> Here the MOF MLCT phosphorescence is quenched by interaction with triplet state molecules, such as dioxygen in its ground state. Due to the high porosity of the MOF, the luminescence intensity changes reversibly upon alteration of the dioxygen concentration (more rapidly than the enzymatic  $\text{O}_2$  consumption rate) and this heterogeneous sensor does not interfere with the enzymatic reaction. Hence, it represents a versatile tool for the kinetic investigation of  $\text{Fe}^{2+}/\alpha$ -KG-dependent dioxygenases allowing for real-time, continuous monitoring. Based on this method, the authors were able to identify lag, linear and non-linear phases of the TET-mediated 5mdC oxidation process. The real-time nature of the assay allowed for relatively accurate determination of reaction velocity in comparison to other more common methods (LC-MS/MS,  $^{14}\text{CO}_2$  radioisotope assay, global

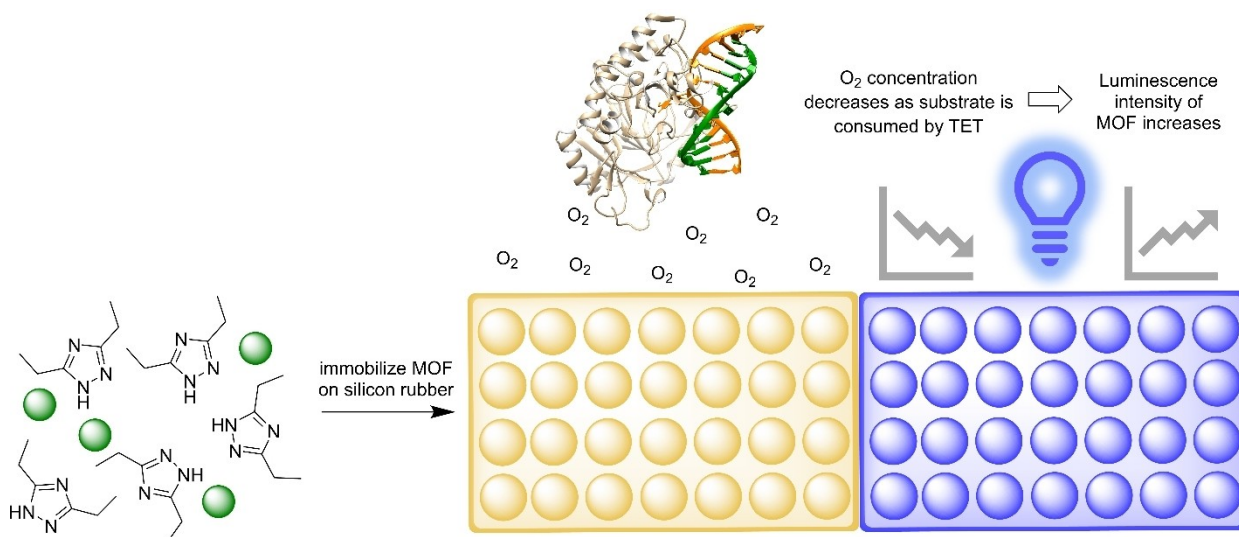


**Figure 11.** Real-time continuous monitoring of TET activity by means of an MOF-based  $O_2$  sensor. After assembly of the MOF from the starting materials (green spheres represent copper ions) on silicone rubber (golden plate) the system exhibits little luminescence due to the quenching by  $O_2$ . As oxygen is consumed during the enzymatic reaction (structural representation of TET is shown as an example, green and orange represent opposite strands of DNA in the substrate), the MOF becomes luminescent (blue plate).

5hmdC quantification), which can only provide average values and are snapshots at certain time points in addition to being more time-consuming. Due to differences in the methods used, distinct  $K_M$  and  $k_{cat}$  values for TET2 towards 5mdC in ssDNA were reported and compared to previous studies,<sup>[13,38b,92]</sup> which also confirmed the finding that TET enzymes only show low sensitivity against  $O_2$  concentration changes.<sup>[92]</sup>

### 3.2.4. Assays based on co-product elimination from the main substrate

As already mentioned above, the AlkB enzyme family produces small organic molecules as side products. Most often, this is formaldehyde (in the case of methylated bases), but more complex aldehydes can be eliminated as well, depending on the structure of the alkyl modification (see Scheme 2). These side products provide viable and reasonably convenient pathways to study enzyme activity. Firstly, short alkyl groups, and especially methyl groups, can easily be artificially introduced into DNA substrates, which is particularly interesting for isotopic and radioactive labelling strategies (see above). Secondly, the highly electrophilic reactivity of aldehydes towards a variety of functionalities, such as amines, hydroxylamines or hydrazines can be exploited in chemical capture approaches. Thirdly, a series of enzymes are known that process the cytotoxin formaldehyde and can be employed for coupled enzymatic assays. Formaldehyde can also be tracked when a  $^{13}C$ -labelled methyl group is incorporated in the substrate. This was demonstrated by Schofield with histone demethylase JMJD2E and labelled tri- and dimethylated peptides and using 1D  $^{13}C$  heteronuclear single quantum coherence (HSQC) NMR spectroscopy.<sup>[84b]</sup>

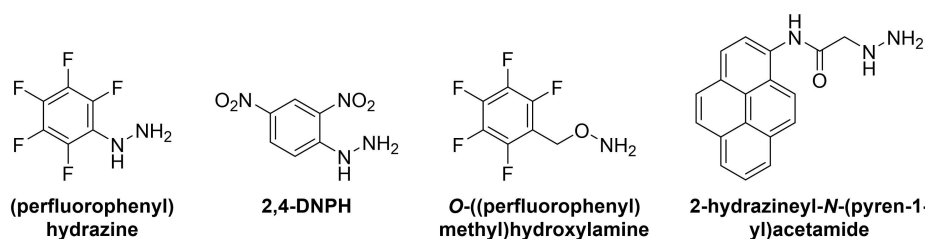
When DNA substrates are artificially (hyper)methylated, radioactive [ $^{14}C$ ]- or [ $^3H$ ]-containing methyl groups can be introduced *via* common methylation agents such as methyl iodide, dimethyl sulphate or methyl nitrosourea. Upon demethylase treatment, they are eliminated as radioactively labelled formaldehyde, which can be quantified by scintillation counting after DNA precipitation. This approach was utilized by Sedgwick, Hausinger *et al.*, in combination with other strategies, to test EcAlkB activity against randomly [ $^{14}C$ ]-methylated poly(dA) and poly(dC) oligonucleotides.<sup>[20d]</sup> In a comparative study of EcAlkB and its human homologues hAlkBH1, hAlkBH2 and hAlkBH3, [ $^{14}C$ ]-methyl groups were introduced as well.<sup>[22a]</sup> While hAlkBH1 appeared active on neither 1mdA nor 3mdC, hAlkBH2 and hAlkBH3 repaired both lesions in single-stranded and double-stranded DNA, although with different substrate preference. Another group proposed that hAlkBH2 prefers dsDNA, whereas hAlkBH3 rather requires ssDNA or even RNA,<sup>[22b]</sup> based on [ $^3H$ ]-radioactivity measurements. Subsequently, it was shown that the substrate specificity of hAlkBH2 is dependent on the  $Mg^{2+}$  concentration.<sup>[20e]</sup> EcAlkB, hAlkBH2 and hAlkBH3 were also tested for their demethylation reactivity towards 3mT.<sup>[20h]</sup> Later, Krokan and co-workers reported that hAlkBH1 acts even as 3mdC and  $m^3C$  demethylase in mitochondrial DNA and RNA.<sup>[21h]</sup> In conjunction with the 1- [ $^{14}C$ ]-succinate method, radioactive formaldehyde monitoring provided access to the activities of several viral AlkB homologues.<sup>[93]</sup> An assay measuring depletion of a tritiated substrate was further utilized in a detailed study on the structure and function of wildtype hAlkBH3.<sup>[33]</sup>

When aldehydes react with hydroxylamines or hydrazines, oximes and hydrazones, respectively, are virtually quantitatively formed. This chemical behavior was exploited by Sedgwick, Hausinger *et al.* when they subjected unlabeled hypermethylated poly(dA) and poly(dC) oligonucleotides to EcAlkB

treatment.<sup>[20d]</sup> Their protocol involved the capture of formaldehyde with (pentafluorophenyl)hydrazine (Scheme 5) and quantification of this adduct *via* GC-MS analysis. The chemical derivatization approach can also be merged with other strategies. This is exemplified by Sedgwick *et al.* who studied EcAlkB activity on 1mdA, 3mdC and 1-ethylDA by condensation of [<sup>14</sup>C]-formaldehyde or [<sup>14</sup>C]-acetaldehyde with 2,4-DNPH (Scheme 5), followed by HPLC analysis and scintillation counting.<sup>[22a]</sup> Another common reagent for derivatization prior to GC-MS analysis is *O*-(pentafluorobenzyl)hydroxylamine (Scheme 5) that has been applied in a kinetic investigation of EcAlkB DNA repair.<sup>[80b]</sup> Even though not an elimination product, aldehyde reactivity towards hydrazines has further been made use of in an *in vitro* study on whether iterative TET1 oxidation of cytosine 5-substituents occurs in a consecutive or rather a distributive manner.<sup>[103]</sup> Therefore, a chemical probe reagent containing an aldehyde-sensitive hydrazine moiety, to react with the TET intermediate 5fdC, and a fluorescent pyrene

function was utilized (2-hydrazineyl-*N*-(pyren-1-yl)acetamide, Scheme 5).

The high reactivity against *N*-nucleophiles makes formaldehyde a potent cytotoxin. Since several metabolic pathways yield formaldehyde as byproduct, many organisms possess formaldehyde dehydrogenases (FDHs), rendering it harmless by oxidation.<sup>[104]</sup> The redox co-factor NAD<sup>+</sup> is simultaneously reduced to NADH which shows fluorescence at around 460 nm.<sup>[105]</sup> Thus, kinetic assays coupling nucleic acid demethylase activity to formaldehyde oxidation are viable, which was, for instance, exploited by Sedgwick, Hausinger *et al.*<sup>[20d]</sup> Roy and Bhagwat later achieved advancement in terms of sensitivity of that assay.<sup>[106]</sup> They exchanged the redox co-factor NAD<sup>+</sup> by 3-acetylpyridine adenine dinucleotide (APAD<sup>+</sup>) and reached a 30 times higher extinction coefficient with a slight shift of excitation and luminescence wavelengths (363 nm and 482 nm, respectively), which allows working with sub-nanomole amounts of methylated substrate. With this assay, they investigated Michaelis-Menten kinetics of EcAlkB towards 1mdA



**Scheme 5.** Different hydrazines and hydroxylamines that have been used to capture formaldehyde or derivatize other molecules of interest with aldehyde functional groups such as 5fC. The abbreviation of 2,4-dinitrophenylhydrazine (2,4-DNPH) is indicated as this structure was mentioned regularly in this text.

Table 2. Summary of methods discussed in section 2 of this review with selected accessible features of the system of interest.		
Characterization method	Type of information gained	Advantages/disadvantages/comments
X-ray crystallography	Molecular structural details of substrate recognition	Applicable for resting state (inhibitor might be needed); requires crystals; sometimes <i>in crystallo</i> reactions possible to track intermediate species
NMR spectroscopy	Changes in flexibility/rigidity of entire protein upon substrate and co-factor or product binding and release	Size limitation for protein; isotope labelling often necessary
EPR spectroscopy	Coordination environment of metal in the active site (e.g. Number of N-donor atoms bound to metal), geometry	Fe <sup>2+</sup> difficult to observe without highly specialized equipment, thus Cu <sup>2+</sup> often used instead
Fluorescence spectroscopy	Local protein dynamics, folding and substrate binding	Fluorescent labels or antenna features need to be present on enzyme or substrate; thermodynamic and kinetic information (combined with stopped flow) accessible
Isothermal titration calorimetry	Thermodynamics of metal and substrate binding to protein, binding constants, and kinetics of substrate turnover	No labels necessary
CD spectroscopy	Thermal stability of protein, changes in secondary and tertiary structure upon substrate or co-factor binding	Additives (e.g. buffer, or ascorbate) can obscure signal
UV/Vis spectroscopy	Information on active site features (binding of $\alpha$ -KG to Fe <sup>2+</sup> ) by e.g. monitoring MLCT absorption bands	Kinetic information (combined with stopped flow) on rise and decay of certain intermediates accessible.
SPR spectroscopy	Real-time and label-free detection of biomolecular interactions to determine thermodynamic and kinetic parameters	Tag or label on protein or substrate for immobilization necessary; interaction can be studied under changing conditions

and 3mdC and obtained markedly distinct values than from previous studies,<sup>[20e,107]</sup> that they attributed to differences in DNA substrate sequence and secondary structure formation. They additionally noticed that Tris can serve as substrate for FDH and is thus an unsuitable buffer component for this type of assay. Further, it should be noted that Tris can react with formaldehyde itself in a Schiff base reaction.<sup>[108]</sup>

#### 4. Conclusion

The study of DNA and RNA repair and modification mechanisms, both in and outside of epigenetics context, has seen remarkable progress in the last years. The collective effort of researchers across a broad range of disciplines, from biochemistry to inorganic chemistry, has led to a fair understanding of the mode of action of EcAlkB, AlkBH, TET and many other enzymes. However, these studies often apply a limited number of specific methods which has created “white spots” on the map of enzymatic DNA modification and repair. In addition, detailed mechanistic understanding has mostly been extrapolated from TauD (using Mössbauer and MCD among other methods). By collecting a comprehensive overview on used methods (Table 2) as well as the most recent information in this review, we hope to address this and give researchers in the field the opportunity to learn about available spectroscopic methods and assay setups that would be complementary and useful for their studies. One problem is the multitude of techniques that make it difficult to directly compare *e.g.* kinetic parameters from different studies. In addition, one recognized major pitfall in working with isolated Fe<sup>2+</sup>/ $\alpha$ -KG-dependent enzymes is their notorious ability to autoxidize and self-hydroxylate in the presence of molecular dioxygen but absence of substrate. Since *in vivo* tissue oxygen levels are generally low, better regulated and controlled, it stands to question how kinetic parameters determined *in vitro* reflect the *in vivo* situation. Thus, these results should always be interpreted with caution.

#### Author contributions

All authors were involved in literature search, review and writing of this manuscript.

#### Acknowledgements

The authors thank Angie Kirchner, Karina Betuker and Katie Fisher for proofreading. A grant from the Deutsche Forschungsgemeinschaft (DFG, German Research Foundation) – SFB 1309-325871075 is gratefully acknowledged. N.S.W.J. acknowledges financial support by the Studienstiftung des Deutschen Volkes and the Joachim Herz Stiftung. Open Access funding enabled and organized by Projekt DEAL.

#### Conflict of Interest

The authors declare no conflict of interest.

**Keywords:** AlkBH · DNA methylation · epigenetics · spectroscopy · TET enzymes

- [1] a) O. Hayaishi, M. Katagiri, S. Rothberg, *J. Am. Chem. Soc.* **1955**, *77*, 5450–5451; b) H. S. Mason, W. L. Fowlks, E. Peterson, *J. Am. Chem. Soc.* **1955**, *77*, 2914–2915.
- [2] a) H. Hanauske-Abel, V. Günzler, *J. Theor. Biol.* **1982**, *94*, 421–455; b) J. C. Price, E. W. Barr, B. Tirupati, J. M. Bollinger, C. Krebs, *Biochemistry* **2003**, *42*, 7497–7508; c) J. C. Price, E. W. Barr, T. E. Glass, C. Krebs, J. M. Bollinger, *J. Am. Chem. Soc.* **2003**, *125*, 13008–13009; d) D. A. Proshlyakov, T. F. Henshaw, G. R. Monterosso, M. J. Ryle, R. P. Hausinger, *J. Am. Chem. Soc.* **2004**, *126*, 1022–1023; e) J. C. Price, E. W. Barr, L. M. Hoffart, C. Krebs, J. M. Bollinger, *Biochemistry* **2005**, *44*, 8138–8147.
- [3] a) S. Goudarzi, S. R. Iyer, J. T. Babicz, J. J. Yan, G. H. J. Peters, H. E. M. Christensen, B. Hedman, K. O. Hodgson, E. I. Solomon, *Proc. Natl. Acad. Sci. USA* **2020**, *117*, 5152–5159; b) E. I. Solomon, K. M. Light, L. V. Liu, M. Srnc, S. D. Wong, *Acc. Chem. Res.* **2013**, *46*, 2725–2739.
- [4] M. J. Ryle, R. Padmakumar, R. P. Hausinger, *Biochemistry* **1999**, *38*, 15278–15286.
- [5] J. C. Price, E. W. Barr, B. Tirupati, J. M. Bollinger Jr., C. Krebs, *Biochemistry* **2003**, *42*, 7497–7508.
- [6] D. A. Proshlyakov, J. McCracken, R. P. Hausinger, *J. Biol. Inorg. Chem.* **2017**, *22*, 367–379.
- [7] P. J. Riggs-Gelasco, J. C. Price, R. B. Guyer, J. H. Brehm, E. W. Barr, J. M. Bollinger, C. Krebs, *J. Am. Chem. Soc.* **2004**, *126*, 8108–8109.
- [8] E. L. Hegg, L. Que Jr., *Eur. J. Biochem.* **1997**, *250*, 625–629.
- [9] P. K. Grzyska, E. H. Appelman, R. P. Hausinger, D. A. Proshlyakov, *Proc. Natl. Acad. Sci. USA* **2010**, *107*, 3982–3987.
- [10] S. Sinnecker, N. Svensen, E. W. Barr, S. Ye, J. M. Bollinger, F. Neese, C. Krebs, *J. Am. Chem. Soc.* **2007**, *129*, 6168–6179.
- [11] J. A. Hangasky, H. Gandhi, M. A. Valliere, N. E. Ostrom, M. J. Knapp, *Biochemistry* **2014**, *53*, 8077–8084.
- [12] a) C. W. John, G. M. Swain, R. P. Hausinger, D. A. Proshlyakov, *J. Phys. Chem.* **2019**, *123*, 7785–7793; b) S. D. Wong, M. Srnc, M. L. Matthews, L. V. Liu, Y. Kwak, K. Park, C. B. Bell III, E. E. Alp, J. Zhao, Y. Yoda, *Nature* **2013**, *499*, 320–323.
- [13] B. Thienpont, J. Steinbacher, H. Zhao, F. D’Anna, A. Kuchnio, A. Ploumakis, B. Ghesquière, L. Van Dyck, B. Boeckx, L. Schoonjans, E. Hermans, F. Amant, V. N. Kristensen, K. P. Koh, M. Mazzone, M. L. Coleman, T. Carell, P. Carmeliet, D. Lambrechts, *Nature* **2016**, *537*, 63–68.
- [14] R. Ougland, T. Rognes, A. Klungland, E. Larsen, *J. Mol. Cell Biol.* **2015**, *7*, 494–504.
- [15] M. G. Vander Heiden, L. C. Cantley, C. B. Thompson, *Science* **2009**, *324*, 1029–1033.
- [16] a) S. Nowicki, E. Gottlieb, *FEBS J.* **2015**, *282*, 2796–2805; b) M. Yang, T. Soga, P. J. Pollard, *J. Clin. Invest.* **2013**, *123*, 3652–3658.
- [17] L. Dang, D. W. White, S. Gross, B. D. Bennett, M. A. Bittinger, E. M. Driggers, V. R. Fantin, H. G. Jang, S. Jin, M. C. Keenan, K. M. Marks, R. M. Prins, P. S. Ward, K. E. Yen, L. M. Liau, J. D. Rabinowitz, L. C. Cantley, C. B. Thompson, M. G. Vander Heiden, S. M. Su, *Nature* **2009**, *462*, 739–744.
- [18] W. Xu, H. Yang, Y. Liu, Y. Yang, P. Wang, S. H. Kim, S. Ito, C. Yang, P. Wang, M. T. Xiao, L. X. Liu, W. Q. Jiang, J. Liu, J. Y. Zhang, B. Wang, S. Frye, Y. Zhang, Y. H. Xu, Q. Y. Lei, K. L. Guan, S. M. Zhao, Y. Xiong, *Cancer Cell* **2011**, *19*, 17–30.
- [19] a) I. Martinez-Reyes, N. S. Chandel, *Nat. Commun.* **2020**, *11*, 102; b) H. Yang, H. Lin, H. Xu, L. Zhang, L. Cheng, B. Wen, J. Shou, K. Guan, Y. Xiong, D. Ye, *Cell Res.* **2014**, *24*, 1017–1020.
- [20] a) V. Koliadenko, T. Wilanowski, *Free Radical Biol. Med.* **2020**, *146*, 1–15; b) T. Sun, R. Wu, L. Ming, *Biomed. Pharmacother.* **2019**, *112*, 108613; c) P. Ø Falnes, R. F. Johansen, E. Seeberg, *Nature* **2002**, *419*, 178–182; d) S. C. Treweek, T. F. Henshaw, R. P. Hausinger, T. Lindahl, B. Sedgwick, *Nature* **2002**, *419*, 174–178; e) P. Ø Falnes, M. Bjørås, P. A. Aas, O. Sundheim, E. Seeberg, *Nucleic Acids Res.* **2004**, *32*, 3456–3461; f) P. V. Afonine, R. W. Grosse-Kunstleve, N. Echols, J. J. Headd, N. W. Moriarty,

- M. Mustyakimov, T. C. Terwilliger, A. Urzhumtsev, P. H. Zwart, P. D. Adams, *Acta Crystallogr. Sect. D* **2012**, *68*, 352–367; g) A. M. Maciejewska, J. Poznański, Z. Kaczmarek, B. Krowisz, J. Niemiński, A. Polkowska-Nowakowska, E. Grzesiuk, J. T. Kuśmierz, *J. Biol. Chem.* **2013**, *288*, 432–441; h) P. Koivisto, P. Robins, T. Lindahl, B. Sedgwick, *J. Biol. Chem.* **2004**, *279*, 40470–40474; i) R. Ougland, C. M. Zhang, A. Liiv, R. F. Johansen, E. Seeberg, Y. M. Hou, J. Remme, P. O. Falnes, *Mol. Cell* **2004**, *16*, 107–116.
- [21] a) R. Ougland, D. Lando, I. Jonson, J. A. Dahl, M. N. Moen, L. M. Nordstrand, T. Rognes, J. T. Lee, A. Klungland, T. Kouzarides, *Stem Cells* **2012**, *30*, 2672–2682; b) R. Ougland, I. Jonson, M. N. Moen, G. Nesse, G. Asker, A. Klungland, E. Larsen, *Cell. Physiol. Biochem.* **2016**, *38*, 173–184; c) T. P. Wu, T. Wang, M. G. Seetin, Y. Lai, S. Zhu, K. Lin, Y. Liu, S. D. Byrum, S. G. Mackintosh, M. Zhong, *Nature* **2016**, *532*, 329–333; d) M. Zhang, S. Yang, R. Nelakanti, W. Zhao, G. Liu, Z. Li, X. Liu, T. Wu, A. Xiao, H. Li, *Cell Res.* **2020**, *30*, 197–210; e) F. Liu, W. Clark, G. Luo, X. Wang, Y. Fu, J. Wei, X. Wang, Z. Hao, Q. Dai, G. Zheng, *Cell* **2016**, *167*, 816–828; f) A. R. Walker, P. Silvestrov, T. A. Müller, R. H. Podolsky, G. Dyson, R. P. Hausinger, G. A. Cisneros, *PLoS Comput. Biol.* **2017**, *13*, e1005345; g) T. A. Müller, M. M. Andzejak, R. P. Hausinger, *Biochem. J.* **2013**, *452*, 509–518; h) M. P. Westbye, E. Feysi, P. A. Aas, C. B. Vågbo, V. A. Talstad, B. Kavli, L. Hagen, O. Sundheim, M. Akbari, N.-B. Liabakk, G. Slupphaug, M. Otterlei, H. E. Krokan, *J. Biol. Chem.* **2008**, *283*, 25046–25056; i) S. Haag, K. E. Sloan, N. Ranjan, A. S. Warda, J. Kretschmer, C. Blessing, B. Hübner, J. Seikowski, S. Dennerlein, P. Rehling, *EMBO J.* **2016**, *35*, 2104–2119.
- [22] a) T. Duncan, S. C. Trewick, P. Koivisto, P. A. Bates, T. Lindahl, B. Sedgwick, *Proc. Natl. Acad. Sci. USA* **2002**, *99*, 16660–16665; b) P. A. Aas, M. Otterlei, P. Ø Falnes, C. B. Vågbo, F. Skorpen, M. Akbari, O. Sundheim, M. Bjørås, G. Slupphaug, E. Seeberg, H. E. Krokan, *Nature* **2003**, *421*, 859–863; c) J. Ringvoll, L. M. Nordstrand, C. B. Vågbo, V. Talstad, K. Reite, P. A. Aas, K. H. Lauritzen, N. B. Liabakk, A. Bjørk, R. W. Doughty, *EMBO J.* **2006**, *25*, 2189–2198; d) K. Bian, S. A. Lenz, Q. Tang, F. Chen, R. Qi, M. Jost, C. L. Drennan, J. M. Essigmann, S. D. Wetmore, D. Li, *Nucleic Acids Res.* **2019**, *47*, 5522–5529; e) Z. Chen, M. Qi, B. Shen, G. Luo, Y. Wu, J. Li, Z. Lu, Z. Zheng, Q. Dai, H. Wang, *Nucleic Acids Res.* **2019**, *47*, 2533–2545.
- [23] a) Y. Ueda, I. Ooshio, Y. Fusamae, K. Kitae, M. Kawaguchi, K. Jingushi, H. Hase, K. Harada, K. Hirata, K. Tsujikawa, *Sci. Rep.* **2017**, *7*, 42271; b) S. Dango, N. Mosammamaparast, M. E. Sowa, L.-J. Xiong, F. Wu, K. Park, M. Rubin, S. Gygi, J. W. Harper, Y. Shi, *Mol. Cell* **2011**, *44*, 373–384; c) X. Li, X. Xiong, K. Wang, L. Wang, X. Shu, S. Ma, C. Yi, *Nat. Chem. Biol.* **2016**, *12*, 311–316; d) N. Tsao, J. R. Brickner, R. Rodell, A. Ganguly, M. Wood, C. Oyeniran, T. Ahmad, H. Sun, A. Bacolla, L. Zhang, *Mol. Cell* **2021**, *81*, 4228–4242, e4228.
- [24] a) V. Rajicka, T. Skalicky, S. Vanacova, *Biochim. Biophys. Acta* **2019**, *1862*, 343–355; b) J. Wang, J. Wang, Q. Gu, Y. Ma, Y. Yang, J. Zhu, Q. a Zhang, *Cancer Cell Int.* **2020**, *20*, 1–7; c) S. Zhang, B. S. Zhao, A. Zhou, K. Lin, S. Zheng, Z. Lu, Y. Chen, E. P. Sulman, K. Xie, O. Böglér, *Cancer Cell* **2017**, *31*, 591–606, e596; d) G. Zheng, J. A. Dahl, Y. Niu, P. Fedorcsak, C.-M. Huang, C. J. Li, C. B. Vågbo, Y. Shi, W.-L. Wang, S.-H. Song, *Mol. Cell* **2013**, *49*, 18–29; e) J. D. Toh, S. W. Crossley, K. J. Bruemmer, J. G. Eva, D. He, D. A. Iovan, C. J. Chang, *Proc. Natl. Acad. Sci. USA* **2020**, *117*, 25284–25292.
- [25] a) Y. Fu, Q. Dai, W. Zhang, J. Ren, T. Pan, C. He, *Angew. Chem. Int. Ed.* **2010**, *49*, 8885–8888; *Angew. Chem.* **2010**, *122*, 9069–9072; b) E. Van den Born, C. B. Vågbo, L. Songe-Møller, V. Leihne, G. F. Lien, G. Leszczynska, A. Malkiewicz, H. E. Krokan, F. Kirpekar, A. Klungland, *Nat. Commun.* **2011**, *2*, 1–7; c) L. Songe-Møller, E. van den Born, V. Leihne, C. B. Vågbo, T. Kristoffersen, H. E. Krokan, F. Kirpekar, P. Ø Falnes, A. Klungland, *Mol. Cell. Biochem.* **2010**, *30*, 1814–1827.
- [26] a) M. Bartosovic, H. C. Molares, P. Gregorova, D. Hrossova, G. Kudla, S. Vanacova, *Nucleic Acids Res.* **2017**, *45*, 11356–11370; b) G. Jia, Y. Fu, X. Zhao, Q. Dai, G. Zheng, Y. Yang, C. Yi, T. Lindahl, T. Pan, Y.-G. Yang, C. He, *Nat. Chem. Biol.* **2011**, *7*, 885–887; c) G. Jia, C.-G. Yang, S. Yang, X. Jian, C. Yi, Z. Zhou, C. He, *FEBS Lett.* **2008**, *582*, 3313–3319; d) Z. Li, H. Weng, R. Su, X. Weng, Z. Zuo, C. Li, H. Huang, S. Nachtergaele, L. Dong, C. Hu, X. Qin, L. Tang, Y. Wang, G.-M. Hong, H. Huang, X. Wang, P. Chen, S. Gurbuxani, S. Arnovitz, Y. Li, S. Li, J. Strong, M. B. Neilly, R. A. Larson, X. Jiang, P. Zhang, J. Jin, C. He, J. Chen, *Cancer Cell* **2017**, *31*, 127–141.
- [27] a) S. Ito, L. Shen, Q. Dai, S. C. Wu, L. B. Collins, J. A. Swenberg, C. He, Y. Zhang, *Science* **2011**, *333*, 1300–1303; b) M. Tahiliani, K. P. Koh, Y. Shen, W. A. Pastor, H. Bandukwala, Y. Brudno, S. Agarwal, L. M. Iyer, D. R. Liu, L. Aravind, A. Rao, *Science* **2009**, *324*, 930–935; c) Y.-F. He, B.-Z. Li, Z. Li, P. Liu, Y. Wang, Q. Tang, J. Ding, Y. Jia, Z. Chen, L. Li, Y. Sun, X. Li, Q. Dai, C.-X. Song, K. Zhang, C. He, G.-L. Xu, *Science* **2011**, *333*, 1303–1307; d) J. Lan, N. Rajan, M. Bizet, A. Penning, N. K. Singh, D. Guallar, E. Calonne, A. L. Greci, E. Bonvin, R. Depluis, P. J. Hsu, S. Nachtergaele, C. Ma, R. Song, A. Fuentes-Iglesias, B. Hassabi, P. Putmans, F. Mies, G. Menschaert, J. J. L. Wong, M. Fidalgo, B. Yuan, F. Fuks, *Nat. Commun.* **2020**, *11*, 1–15.
- [28] Z. Lin, X. Wang, K. A. Bustin, K. Shishikura, N. R. McKnight, L. He, R. M. Suci, K. Hu, X. Han, M. Ahmadi, *ACS Cent. Sci.* **2021**, *7*, 1524–1534.
- [29] a) B. I. Fedele, V. Singh, J. C. Delaney, D. Li, J. M. Essigmann, *J. Biol. Chem.* **2015**, *290*, 20734–20742; b) L. F. Wu, S. Meng, G. L. Tang, *Biochim. Biophys. Acta Proteins Proteomics* **2016**, *1864*, 453–470.
- [30] a) P. J. Holland, T. Hollis, *PLoS One* **2010**, *5*, e8680; b) C. Yi, G. Jia, G. Hou, Q. Dai, W. Zhang, G. Zheng, X. Jian, C. G. Yang, Q. Cui, C. He, *Nature* **2010**, *468*, 330–333; c) B. Yu, W. C. Edstrom, J. Benach, Y. Hamuro, P. C. Weber, B. R. Gibney, J. F. Hunt, *Nature* **2006**, *439*, 879–884; d) B. Yu, J. F. Hunt, *Proc. Natl. Acad. Sci. USA* **2009**, *106*, 14315–14320; e) C. Yi, B. Chen, B. Qi, W. Zhang, G. Jia, L. Zhang, C. J. Li, A. R. Dinner, C.-G. Yang, C. He, *Nat. Struct. Mol. Biol.* **2012**, *19*, 671–676; f) E. C. Woon, M. Demetriades, E. A. Bagg, W. Aik, S. M. Krylova, J. H. Ma, M. Chan, L. J. Walport, D. W. Wegman, K. N. Dack, M. A. McDonough, S. N. Krylov, C. J. Schofield, *J. Med. Chem.* **2012**, *55*, 2173–2184; g) R. J. Hopkinson, A. Tumber, C. Yapp, R. Chowdhury, W. Aik, K. H. Che, X. S. Li, J. B. L. Kristensen, O. N. F. King, M. C. Chan, K. K. Yeoh, H. Choi, L. J. Walport, C. C. Thinnis, J. T. Bush, C. Lejeune, A. M. Ryzdik, N. R. Rose, E. A. Bagg, M. A. McDonough, T. Krojer, W. W. Yue, S. S. Ng, L. Olsen, P. E. Brennan, U. Oppermann, S. Muller-Knapp, R. J. Klose, P. J. Ratcliffe, C. J. Schofield, A. Kawamura, *Chem. Sci.* **2013**, *4*, 3110–3117; h) C. Zhu, C. Yi, *Angew. Chem. Int. Ed. Engl.* **2014**, *53*, 3659–3662; i) Q. Li, Y. Huang, X. Liu, J. Gan, H. Chen, C. G. Yang, *J. Biol. Chem.* **2016**, *291*, 11083–11093.
- [31] L. F. Tian, Y. P. Liu, L. Chen, Q. Tang, W. Wu, W. Sun, Z. Chen, X. X. Yan, *Cell Res.* **2020**, *30*, 272–275.
- [32] a) C. G. Yang, C. Yi, E. M. Duguid, C. T. Sullivan, X. Jian, P. A. Rice, C. He, *Nature* **2008**, *452*, 961–965; b) L. Lu, C. Yi, X. Jian, G. Zheng, C. He, *Nucleic Acids Res.* **2010**, *38*, 4415–4425.
- [33] O. Sundheim, C. B. Vagbo, M. Bjaras, M. M. Sousa, V. Talstad, P. A. Aas, F. Drablos, H. E. Krokan, J. A. Tainer, G. Slupphaug, *EMBO J.* **2006**, *25*, 3389–3397.
- [34] a) W. Aik, J. S. Scotti, H. Choi, L. Gong, M. Demetriades, C. J. Schofield, M. A. McDonough, *Nucleic Acids Res.* **2014**, *42*, 4741–4754; b) W. Chen, L. Zhang, G. Zheng, Y. Fu, Q. Ji, F. Liu, H. Chen, C. He, *FEBS Lett.* **2014**, *588*, 892–898; c) C. Feng, Y. Liu, G. Wang, Z. Deng, Q. Zhang, W. Wu, Y. Tong, C. Cheng, Z. Chen, *J. Biol. Chem.* **2014**, *289*, 11571–11583.
- [35] C. Pastore, I. Topalidou, F. Forouhar, A. C. Yan, M. Levy, J. F. Hunt, *J. Biol. Chem.* **2012**, *287*, 2130–2143.
- [36] a) W. Aik, M. Demetriades, M. K. Hamdan, E. A. Bagg, K. K. Yeoh, C. Lejeune, Z. Zhang, M. A. McDonough, C. J. Schofield, *J. Med. Chem.* **2013**, *56*, 3680–3688; b) Z. Han, T. Niu, J. Chang, X. Lei, M. Zhao, Q. Wang, W. Cheng, J. Wang, Y. Feng, J. Chai, *Nature* **2010**, *464*, 1205–1209; c) Y. Huang, J. Yan, Q. Li, J. Li, S. Gong, H. Zhou, J. Gan, H. Jiang, G. F. Jia, C. Luo, C. G. Yang, *Nucleic Acids Res.* **2015**, *43*, 373–384; d) S. Peng, W. Xiao, D. Ju, B. Sun, N. Hou, Q. Liu, Y. Wang, H. Zhao, C. Gao, S. Zhang, R. Cao, P. Li, H. Huang, Y. Ma, Y. Wang, W. Lai, Z. Ma, W. Zhang, S. Huang, H. Wang, Z. Zhang, L. Zhao, T. Cai, Y. L. Zhao, F. Wang, Y. Nie, G. Zhi, Y. G. Yang, E. E. Zhang, N. Huang, *Sci. Transl. Med.* **2019**, *11*, eaau7116; e) J. D. W. Toh, L. Sun, L. Z. M. Lau, J. Tan, J. J. A. Low, C. W. Q. Tang, E. J. Y. Cheong, M. J. H. Tan, Y. Chen, W. Hong, Y. G. Gao, E. C. Y. Woon, *Chem. Sci.* **2015**, *6*, 112–122; f) T. Wang, T. Hong, Y. Huang, H. Su, F. Wu, Y. Chen, L. Wei, W. Huang, X. Hua, Y. Xia, J. Xu, J. Gan, B. Yuan, Y. Feng, X. Zhang, C. G. Yang, X. Zhou, *J. Am. Chem. Soc.* **2015**, *137*, 13736–13739; g) X. Zhang, L. H. Wei, Y. Wang, Y. Xiao, J. Liu, W. Zhang, N. Yan, G. Amu, X. Tang, L. Zhang, G. Jia, *Proc. Natl. Acad. Sci. USA* **2019**, *116*, 2919–2924.
- [37] a) H. Hashimoto, J. E. Pais, N. Dai, I. R. Correa Jr., X. Zhang, Y. Zheng, X. Cheng, *Nucleic Acids Res.* **2015**, *43*, 10713–10721; b) H. Hashimoto, J. E. Pais, X. Zhang, L. Saleh, Z. Q. Fu, N. Dai, I. R. Correa Jr., Y. Zheng, X. Cheng, *Nature* **2014**, *506*, 391–395.
- [38] a) L. Hu, Z. Li, J. Cheng, Q. Rao, W. Gong, M. Liu, Y. G. Shi, J. Zhu, P. Wang, Y. Xu, *Cell* **2013**, *155*, 1545–1555; b) L. Hu, J. Lu, J. Cheng, Q. Rao, Z. Li, H. Hou, Z. Lou, L. Zhang, W. Li, W. Gong, M. Liu, C. Sun, X. Yin, J. Li, X. Tan, P. Wang, Y. Wang, D. Fang, Q. Cui, P. Yang, C. He, H. Jiang, C. Luo, Y. Xu, *Nature* **2015**, *527*, 118–122.
- [39] a) S. G. Jin, Z. M. Zhang, T. L. Dunwell, M. R. Harter, X. Wu, J. Johnson, Z. Li, J. Liu, P. E. Szabo, Q. Lu, G. L. Xu, J. Song, G. P. Pfeifer, *Cell Rep.*

- 2016, 14, 493–505; b) Y. Xu, C. Xu, A. Kato, W. Tempel, J. G. Abreu, C. Bian, Y. Hu, D. Hu, B. Zhao, T. Cerovina, J. Diao, F. Wu, H. H. He, Q. Cui, E. Clark, C. Ma, A. Barbara, G. J. Veenstra, G. Xu, U. B. Kaiser, X. S. Liu, S. P. Sugrue, X. He, J. Min, Y. Kato, Y. G. Shi, *Cell* **2012**, 151, 1200–1213.
- [40] B. Xu, D. Liu, Z. Wang, R. Tian, Y. Zuo, *Cell. Mol. Life Sci.* **2020**.
- [41] K. Al-Qahtani, B. Jabeen, R. Sekirnik, N. Riaz, T. D. W. Claridge, C. J. Schofield, J. S. O. McCullagh, *Phytochemistry* **2015**, 117, 456–461.
- [42] G. Wang, Q. He, C. Feng, Y. Liu, Z. Deng, X. Qi, W. Wu, P. Mei, Z. Chen, *J. Biol. Chem.* **2014**, 289, 27924–27936.
- [43] S. Harteis, S. Schneider, *Int. J. Mol. Sci.* **2014**, 15, 12335–12363.
- [44] a) N. Liu, Q. Dai, G. Zheng, C. He, M. Parisien, T. Pan, *Nature* **2015**, 518, 560–564; b) C. Roost, S. R. Lynch, P. J. Batista, K. Qu, H. Y. Chang, E. T. Kool, *J. Am. Chem. Soc.* **2015**, 137, 2107–2115.
- [45] C. Rauch, M. Trieb, B. Wellenzohn, M. Loferer, A. Voegelé, F. R. Wibowo, K. R. Liedl, *J. Am. Chem. Soc.* **2003**, 125, 14990–14991.
- [46] C. Acosta-Silva, V. Branchadell, J. Bertran, A. Oliva, *J. Phys. Chem. B* **2010**, 114, 10217–10227.
- [47] C. B. Mulholland, F. R. Traube, E. Ugru, E. Parsa, E. M. Eckl, M. Schonung, M. Modic, M. D. Bartoschek, P. Stolz, J. Ryan, T. Carell, H. Leonhardt, S. Bultmann, *Sci. Rep.* **2020**, 10, 12066.
- [48] B. Bleijlevens, T. Shivarattan, E. Flashman, Y. Yang, P. J. Simpson, P. Koivisto, B. Sedgwick, C. J. Schofield, S. J. Matthews, *EMBO Rep.* **2008**, 9, 872–877.
- [49] B. Bleijlevens, T. Shivarattan, K. S. van den Boom, A. de Haan, G. van der Zwan, P. J. Simpson, S. J. Matthews, *Biochemistry* **2012**, 51, 3334–3341.
- [50] D. P. Frueh, A. C. Goodrich, S. H. Mishra, S. R. Nichols, *Curr. Opin. Struct. Biol.* **2013**, 23, 734–739.
- [51] B. Ergel, M. L. Gill, L. Brown, B. Yu, A. G. Palmer, J. F. Hunt, *J. Biol. Chem.* **2014**, 289, 29584–29601.
- [52] B. Bleijlevens, T. Shivarattan, B. Sedgwick, S. E. J. Rigby, S. J. Matthews, *J. Inorg. Biochem.* **2007**, 101, 1043–1048.
- [53] J. Krzystek, A. Ozarowski, J. Telsler, *Coord. Chem. Rev.* **2006**, 250, 2308–2324.
- [54] I. S. MacPherson, M. E. P. Murphy, *Cell. Mol. Life Sci.* **2007**, 64, 2887–2899.
- [55] M. M. Harding, *Acta Crystallogr. Sect. D* **2004**, 60, 849–859.
- [56] C. A. Smith, B. F. Anderson, H. M. Baker, E. N. Baker, *Biochemistry* **1992**, 31, 4527–4533.
- [57] J. Peisach, W. E. Blumberg, *Arch. Biochem. Biophys.* **1974**, 165, 691–708.
- [58] L. Kanazhevskaya, D. Smyshlyayev, I. Alekseeva, O. Fedorova, *Russ. J. Bioorg. Chem.* **2019**, 45, 630–640.
- [59] L. Y. Kanazhevskaya, I. V. Alekseeva, O. S. Fedorova, *Molecules* **2019**, 24, 4576.
- [60] C. C. Gradinaru, D. O. Marushchak, M. Samim, U. J. Krull, *Analyst* **2010**, 135, 452–459.
- [61] a) D. E. Wilcox, *Inorg. Chim. Acta* **2008**, 361, 857–867; b) M. W. Freyer, E. A. Lewis, *Methods Cell Biol.* **2008**, 84, 79–113; c) N. J. Buurma, I. Haq, *Methods* **2007**, 42, 162–172.
- [62] a) M. D. Allen, C. G. Grummitt, C. Hilcenko, S. Y. Min, L. M. Tonkin, C. M. Johnson, S. M. Freund, M. Bycroft, A. J. Warren, *EMBO J.* **2006**, 25, 4503–4512; b) C. Xu, C. Bian, R. Lam, A. Dong, J. Min, *Nat. Commun.* **2011**, 2, 1–8.
- [63] A. K. Singh, B. Zhao, X. Liu, X. Wang, H. Li, H. Qin, X. Wu, Y. Ma, D. Horne, X. Yu, *Proc. Natl. Acad. Sci. USA* **2020**, 117, 3621–3626.
- [64] N. J. Greenfield, *Nat. Protoc.* **2006**, 1, 2876–2890.
- [65] R. P. Hausinger, *Crit. Rev. Biochem. Mol. Biol.* **2004**, 39, 21–68.
- [66] a) M. L. Neidig, C. D. Brown, K. M. Light, D. G. Fujimori, E. M. Nolan, J. C. Price, E. W. Barr, J. M. Bollinger Jr., C. Krebs, C. T. Walsh, E. I. Solomon, *J. Am. Chem. Soc.* **2007**, 129, 14224–14231; b) S. R. Iyer, V. D. Chaplin, M. J. Knapp, E. I. Solomon, *J. Am. Chem. Soc.* **2018**, 140, 11777–11783.
- [67] Y. Mishina, L. X. Chen, C. He, *J. Am. Chem. Soc.* **2004**, 126, 16930–16936.
- [68] M. J. Ryle, A. Liu, R. B. Muthukumar, R. Y. N. Ho, K. D. Koehntop, J. McCracken, L. Que, R. P. Hausinger, *Biochemistry* **2003**, 42, 1854–1862.
- [69] T. F. Henshaw, M. Feig, R. P. Hausinger, *J. Inorg. Biochem.* **2004**, 98, 856–861.
- [70] A. Liu, R. Y. N. Ho, L. Que, M. J. Ryle, B. S. Phinney, R. P. Hausinger, *J. Am. Chem. Soc.* **2001**, 123, 5126–5127.
- [71] R. Bakhtiar, *J. Chem. Educ.* **2013**, 90, 203–209.
- [72] a) S. Kizaki, H. Sugiyama, *Org. Biomol. Chem.* **2014**, 12, 104–107; b) F. Spada, S. Schiffers, A. Kirchner, Y. Zhang, G. Arista, O. Kosmatchev, E. Korytiakova, R. Rahimoff, C. Ebert, T. Carell, *Nat. Chem. Biol.* **2020**, 16, 1411–1419.
- [73] F. R. Traube, S. Schiffers, K. Iwan, S. Kellner, F. Spada, M. Müller, T. Carell, *Nat. Protoc.* **2019**, 14, 283–312.
- [74] a) M. G. Krokidis, M. Louka, E. K. Efthimiadou, S.-K. Zervou, K. Papadopoulos, A. Hiskia, C. Ferreri, C. Chatgialoglou, *Cancers* **2019**, 11, 480; b) J.-B. Alberge, F. Magrangeas, M. Wagner, S. Denié, C. Guérin-Charbonnel, L. Champion, M. Attal, H. Avet-Loiseau, T. Carell, P. Moreau, S. Minvielle, A. A. Sérandour, *Clin. Epigenet.* **2020**, 12, 163.
- [75] D. Schmidl, N. S. W. Jonasson, E. Korytiaková, T. Carell, L. J. Daumann, *Angew. Chem. Int. Ed.* **2021**, 60, 21457–21463.
- [76] A. Hofer, Z. J. Liu, S. Balasubramanian, *J. Am. Chem. Soc.* **2019**, 141, 6420–6429.
- [77] J. P. Patel, M. L. Sowers, J. L. Herring, J. A. Theruvathu, M. R. Emmett, B. E. Hawkins, K. Zhang, D. S. DeWitt, D. S. Prough, L. C. Sowers, *Chem. Res. Toxicol.* **2015**, 28, 2352–2363.
- [78] a) N. S. W. Jonasson, R. Janßen, A. Menke, F. L. Zott, H. Zipse, L. J. Daumann, *ChemBioChem* **2021**, 22, 3333–3340; b) N. S. W. Jonasson, L. J. Daumann, *Chem. Eur. J.* **2019**, 25, 12091–12097.
- [79] B. Yu, J. F. Hunt, *Proc. Natl. Acad. Sci. USA* **2009**, 106, 14315–14320.
- [80] a) V. Singh, B. I. Fedeles, D. Li, J. C. Delaney, I. D. Kozekov, A. Kozekova, L. J. Marnett, C. J. Rizzo, J. M. Essigmann, *Chem. Res. Toxicol.* **2014**, 27, 1619–1631; b) J. C. Delaney, L. Smeester, C. Wong, L. E. Frick, K. Taghizadeh, J. S. Wishnok, C. L. Drennan, L. D. Samson, J. M. Essigmann, *Nat. Struct. Mol. Biol.* **2005**, 12, 855–860; c) L. E. Frick, J. C. Delaney, C. Wong, C. L. Drennan, J. M. Essigmann, *Proc. Natl. Acad. Sci. USA* **2007**, 104, 755–760; d) D. Li, J. C. Delaney, C. M. Page, A. S. Chen, C. Wong, C. L. Drennan, J. M. Essigmann, *J. Nucleic Acids* **2010**, 2010, 369434; e) D. Li, B. I. Fedeles, N. Shrivastav, J. C. Delaney, X. Yang, C. Wong, C. L. Drennan, J. M. Essigmann, *Chem. Res. Toxicol.* **2013**, 26, 1182–1187.
- [81] T. A. Müller, K. Meek, R. P. Hausinger, *DNA Repair* **2010**, 9, 58–65.
- [82] M. R. Baldwin, S. J. Admiraal, P. J. O'Brien, *J. Biol. Chem.* **2020**, 295, 7317–7326.
- [83] a) J. J. Hutton, A. L. Tappel, S. Udenfriend, *Arch. Biochem. Biophys.* **1967**, 118, 231–240; b) R. E. Rhoads, S. Udenfriend, *Proc. Natl. Acad. Sci. USA* **1968**, 60, 1473–1478; c) L. A. McNeill, L. Bethge, K. S. Hewitson, C. J. Schofield, *Anal. Biochem.* **2005**, 336, 125–131; d) L. Luo, M. B. Pappalardi, P. J. Tummino, R. A. Copeland, M. E. Fraser, P. K. Grzyska, R. P. Hausinger, *Anal. Biochem.* **2006**, 353, 69–74; e) H.-J. Lee, M. D. Lloyd, K. Harlos, C. J. Schofield, *Biochem. Biophys. Res. Commun.* **2000**, 267, 445–448.
- [84] a) E. Flashman, L. M. Hoffart, R. B. Hamed, J. M. Bollinger Jr., C. Krebs, C. J. Schofield, *FEBS J.* **2010**, 277, 4089–4099; b) R. J. Hopkinson, R. B. Hamed, N. R. Rose, T. D. Claridge, C. J. Schofield, *ChemBioChem* **2010**, 11, 506–510.
- [85] a) G. Kaule, V. Günzler, *Anal. Biochem.* **1990**, 184, 291–297; b) C. J. Cunliffe, T. J. Franklin, R. M. Gaskell, *Biochem. J.* **1986**, 240, 617–619.
- [86] A. Khan, C. J. Schofield, T. D. Claridge, *ChemBioChem* **2020**, 21, 2898.
- [87] M. A. Martini, O. Rüdiger, N. Breuer, B. Nöring, S. DeBeer, P. Rodríguez-Maciá, J. A. Birrell, *J. Am. Chem. Soc.* **2021**, 143, 18159–18171.
- [88] S. J. Wong, A. E. Ringel, W. Yuan, J. A. Paulo, H. Yoon, M. A. Currie, M. C. Haigis, *J. Biol. Chem.* **2021**, 296, 100397.
- [89] A. Thalhammer, Z. Bencokova, R. Poole, C. Loenarz, J. Adam, L. O'Flaherty, J. Schödel, D. Mole, K. Giaslaktiotis, C. J. Schofield, E. M. Hammond, P. J. Ratcliffe, P. J. Pollard, *PLoS One* **2011**, 6, e16210.
- [90] a) L. Tuderman, R. Myllylä, K. I. Kivirikko, *Eur. J. Biochem.* **1977**, 80, 341–348; b) D. F. Counts, G. J. Cardinale, S. Udenfriend, *Proc. Natl. Acad. Sci. USA* **1978**, 75, 2145–2149.
- [91] V. T. Monsen, O. Sundheim, P. A. Aas, M. P. Westbye, M. M. Sousa, G. Slupphaug, H. E. Krokan, *Nucleic Acids Res.* **2010**, 38, 6447–6455.
- [92] T. Laukka, C. J. Mariani, T. Ihantola, J. Z. Cao, J. Hokkanen, W. G. Kaelin, L. A. Godley, P. Koivunen, *J. Biol. Chem.* **2016**, 291, 4256–4265.
- [93] E. van den Born, M. V. Omelchenko, A. Bekkelund, V. Leihne, E. V. Koonin, V. V. Dolja, P. Ø Falnes, *Nucleic Acids Res.* **2008**, 36, 5451–5461.
- [94] H. Korvald, P. Ø Falnes, J. K. Laerdahl, M. Bjørås, I. Alseth, *DNA Repair* **2012**, 11, 453–462.
- [95] L. G. Bjørnstad, G. Zoppellaro, A. B. Tomter, P. Ø. Falnes, K. K. Andersson, *Biochem. J.* **2011**, 434, 391–398.
- [96] A. B. F. Valle, A. D. Panek, J. R. Mattoon, *Anal. Biochem.* **1978**, 91, 583–599.
- [97] a) S. Burr, A. Caldwell, M. Chong, M. Beretta, S. Metcalf, M. Hancock, M. Arno, S. Balu, V. L. Kropf, R. K. Mistry, A. M. Shah, G. E. Mann, A. C. Brewer, *Nucleic Acids Res.* **2017**, 46, 1210–1226; b) P. Prickaerts, M. E. Adriaens, T. v d Beucken, E. Koch, L. Dubois, V. E. H. Dahlmans, C. Gits, C. T. A. Evelo, M. Chan-Seng-Yue, B. G. Wouters, J. W. Voncken, *Epigenetics Chromatin* **2016**, 9, 46; c) D. Camuzi, I. S. S. de Amorim, L. F.

- Ribeiro Pinto, L. Oliveira Trivilin, A. L. Mencialha, S. C. Soares Lima, *Cells* **2019**, *8*, 300.
- [98] D. D. Shah, J. A. Conrad, B. Heinz, J. M. Brownlee, G. R. Moran, *Biochemistry* **2011**, *50*, 7694–7704.
- [99] L. C. Clark JR, R. Wolf, D. Granger, Z. Taylor, *J. Appl. Physiol.* **1953**, *6*, 189–193.
- [100] A. Ozer, R. K. Bruick, *Nat. Chem. Biol.* **2007**, *3*, 144–153.
- [101] M. Hirsilä, P. Koivunen, V. Günzler, K. I. Kivirikko, J. Myllyharju, *J. Biol. Chem.* **2003**, *278*, 30772–30780.
- [102] Y. Xu, S.-Y. Liu, J. Li, L. Zhang, D. Chen, J.-P. Zhang, Y. Xu, Z. Dai, X. Zou, *Anal. Chem.* **2018**, *90*, 9330–9337.
- [103] L. Xu, Y. C. Chen, J. Chong, A. Fin, L. S. McCoy, J. Xu, C. Zhang, D. Wang, *Angew. Chem.* **2014**, *126*, 11405–11409; *Angew. Chem. Int. Ed.* **2014**, *53*, 11223–11227.
- [104] H. Reingruber, L. B. Pontel, *Curr. Opin. Toxicol.* **2018**, *9*, 28–34.
- [105] a) B. Chance, *Science* **1954**, *120*, 767–775; b) B. Chance, B. Thorell, *Nature* **1959**, *184*, 931–934.
- [106] T. W. Roy, A. S. Bhagwat, *Nucleic Acids Res.* **2007**, *35*, e147–e147.
- [107] P. Koivisto, T. Duncan, T. Lindahl, B. Sedgwick, *J. Biol. Chem.* **2003**, *278*, 44348–44354.
- [108] B. Jahn, N. S. W. Jonasson, H. Hu, H. Singer, A. Pol, N. M. Good, H. J. M. O. den Camp, N. C. Martinez-Gomez, L. J. Daumann, *J. Biol. Inorg. Chem.* **2020**, *25*, 199–212.

---

Manuscript received: November 2, 2021

Revised manuscript received: January 14, 2022

Accepted manuscript online: January 18, 2022